2014

Regulation and Mechanistic Functions of Caspase-9 RNA Splicing

Ngoc T. Vu
Virginia Commonwealth University

Regulation and Mechanistic Functions of Caspase-9 RNA Splicing

A dissertation submitted in partial fulfillment of the requirements for the degree of Doctor of Molecular Biology and Genetics at Virginia Commonwealth University

by

Ngoc Thanh Vu,
Bachelor of Engineering, Vietnam National University, 2009

Director: Charles E. Chalfant, Ph.D.
Professor and Vice Chair, Department of Biochemistry and Molecular Biology

Virginia Commonwealth University
Richmond, Virginia
August, 2014

Acknowledgment

I cannot express enough thanks to my caring, loving and supportive husband, Son Vo. I feel so sorry that you had to sacrifice a wonderful job position and a joyful life in Vietnam to come to the United State with me just because I would like to go the United State to pursue a PhD program in biological sciences.

I also would like to thank my sister, Hanh Vu, to encourage me to come to the United State for graduate study. It was your great passion and enthusiasm in scientific research that highly motivated me to take part in the long and challenging PhD 'journey'.

My completion of this dissertation could not have been accomplished without love and support of my parents and my brother-in-law, Anh Tran during the past four years it has taken me to graduate. To my parents in Vietnam, your encouragement every single time we talk in the phone means a lot to me!

I also wish to thank Dr. Christie for accepting me into the MBG program and Dr. Chalfant for giving me an opportunity to join his lab, training me to become a successful PhD student and teaching me how to be a productive scientist. I truly enjoy every day in the lab and would like to thank all my former and current lab members for their helpful advice, great technical support, big help on manuscript editing and unending effort to 'Americanize' me. To Margaret, Jackie, Alexis and Jenn, I am proud to be a part of the 'oestrogen' group in the lab - Thank you to include me in all of your 'lady' nights!

To my committee meeting members, Dr. Chalfant, Dr. Moran, Dr. Elmore, Dr. Park and Dr. Roesser, your patience and helpful advice on all of my writing and presentation is sincerely appreciated. Thank you for believing I am qualified for graduation even when I am not actually confident about myself.

Last but not least, I am grateful to Dr. Chlebowski and administration staffs in the Biochemistry Department, who are always willing to help me with paperwork during my stay in this department.

Table of Contents

List of Tables

List of Figures

List of Abbreviations

3 prime untranslated region	3'UTR
4-(2-hydroxyethyl)-1-piperazineethanesulfonic acid	HEPES
5 prime untranslated region	5'UTR
Acquired immune deficiency syndrome	AIDS
Anchorage-independent growth	AIG
Apoptotic protease activating factor 1	Apaf-1
Baculoviral inhibitor of apoptosis repeat containing 5	BIRC5
Baculovirus inhibitor of apoptosis repeat	BIR
B-cell-activating factor receptor	BAFF-R
Bovine serum albumin	BSA
Calf-intestinal phosphatase	CIP
Carbobenzoxy-Leu-Leu-leucinal	MG132
Caspase-9a	C9a
Caspase-9b	C9b
Caspase recruitment/Apaf-1 association domain	CARD
Cellular FLICE-like inhibitory protein	c-FLIP

Cellular inhibitor of apoptosis	cIAP
Chemokine receptor type 4	CXCR4
Coimmunoprecipitation	coIP
Complementary deoxyribonucleic acid	cDNA
Control	Con
Death-inducing signaling complex	DISC
Denatured calf-intestinal phosphatase	De-CIP
Deoxyribonucleic acid	DNA
Dulbecco's modified eagle's medium	DMEM
Electrophoretic mobility shift assay	EMSA
Enzyme-linked immunosorbent assay	ELISA
Epidermal growth factor receptor	EGFR
Ethylene-diamine-tetraacetic acid	EDTA
Exon 3 of caspase-9	C9/E3
Fetal bovine serum	FBS
Fluorescein Isothiocyanate	FITC
Growth arrest and DNA damage induced gene-45	GADD45
Heterogeneous nuclear ribonucleoprotein	hnRNP
Human bronchial epithelial primary cells	HBEpC
Human embryonic kidney 293 cell line	HEK 293
Human non-small cell lung adenocarcinoma epithelial cell line	A549 or H838
Hydrochloric acid	HCl
IAP-binding motif	IBM

Immunoglobulin G	IgG
Immunoprecipitation	IP
Inhibition of apoptosis binding domain	IBM
Inhibitor of kappaB alpha	IκB-α
Inhibitor of kappaB kinase	IKK
Intercellular adhesion molecule-1	ICAM-1
Interferon regulatory factor 3	IFR3
Linker region	LR
Lipopolysaccharides	LPS
Lymphotoxin-beta receptor	LTβR
Magnesium chloride	$MgCl_2$
Matrix metalloproteinase	MMP
Mutant form of inhibitor of kappaB alpha (S32A/S36A)	IκB-αS
Mutated/mutant	Mut
Nuclear localization signal	NLS
Non-small cell lung cancer	NSCLC
Non-specific competitors	NSC
Nuclear factor kappa B	NF-κB
Nuclear factor kappaB-inducing kinase	NIK
Nuclear factor-kappaB essential modulator	NEMO
Nuclear localization signals	NLS
Nucleotide triphosphate	NTP
Peptide sequence DYKDDDK	FLAG

Polymerase chain reaction	PCR
Potassium chloride	q-PCR
Protein kinase B	KCl
Quantitative polymerase chain reaction	AKT
Really interesting new gene	RING
Reaper–Hid–Grim	RHG
Receptor activator of nuclear factor kappaB	RANK
Receptor-interacting protein	RIP
Rel homology domain	RHD
Reverse transcription polymerase chain reaction	RT-PCR
Ribonucleic acid	RNA
RNA oligo	RO
Scaffold attachment factor A	SAF-A
Scaffold attachment region	SAR
Second mitochondrial activator of caspase	Smac/DIABLO
Serine protease urokinase-type plasminogen activator	uPA
Small cell lung cancer	SCLC
Small interfering ribonucleic acid	siRNA
Sodium chloride	NaCl
Sodium dodecyl sulfate polyacrylamide gel electrophoresis	SDS-PAGE
Specific competitors	SC
Streptavidin-biotin affinity purification	SBAP
Transactivation domain	TAD

Transfer ribonucleic acid	tRNA
Tris-borate- ethylene-diamine-tetraacetic acid	TBE
Tumor necrosis factor	TNF
Tumor necrosis factor receptor-associated factor 2/3	TRAF2/3
Vascular cell adhesion molecule-1	VCAM-1
Vascular endothelial growth factor	VEGF
Wild-type	WT
X-linked inhibitor of apoptosis	XIAP

Abstract

REGULATION AND MECHANISTIC FUNCTIONS OF CASPASE-9 RNA SPLICING

By Ngoc Thanh Vu, B.Eng.

A dissertation submitted in partial fulfillment of the requirements for the degree of Doctor of Philosophy at Virginia Commonwealth University.

Virginia Commonwealth University, 2014

Major Director: Charles E. Chalfant, Ph.D.
Professor and Vice Chair, Department of Biochemistry and Molecular Biology

Caspase-9 has two splice variants, pro-apoptotic caspase-9a and anti-apoptotic caspase-9b, and dysregulation of caspase-9 splice variant ratio or expression of caspase-9b isoform has been linked to augmentation of the anchorage-independent growth and tumorigenic capacity of non-small cell lung cancer (NSCLC) cells. This study focuses on cell signaling pathway(s) regulating the alternative splicing of caspase-9 pre-mRNA and mechanistic roles of caspase-9b in a certain oncogenic/survival pathway. In regards to the former, we have identified hnRNP U as a novel splice-enhancer associated with exon 3 of caspase-9 (C9/E3). Moreover, hnRNP U binds

specifically to C9/E3 at an RNA *cis*-element previously reported as the binding site for the splicing repressor, hnRNP L. Phosphorylated hnRNP L interferes with hnRNP U for binding to C9/E3, and our results demonstrate the importance of the phosphoinositide 3-kinase/AKT pathway in modulating the association of hnRNP U to C9/E3. Overall, a mechanistic model has been revealed where hnRNP U competes with hnRNP L for C9/E3 binding to enhance the inclusion of the four-exon cassette, and this splice-enhancing effect is blocked by the AKT pathway via phosphorylation of hnRNP L. As to the latter aim, it is unknown about the mechanistic roles of caspase-9b besides the inhibitory effect on caspase-9a processing. In this study, caspase-9b has been demonstrated to have a dual function in regulating the survival/oncogenic nuclear factor κB (NF-κB) pathway, which is independent from modulating caspase-9a activation. In particular, caspase-9b has been shown to activate the canonical arm and inhibit the non-canonical arm of the NF-κB pathway by destabilizing NF-κB inhibitor alpha (IκB-α) and NF-κB-inducing kinase (NIK). Importantly, this new role for caspase-9b contributes to the enhanced survival and anchorage-independent growth of NSCLC cells conferred by caspase-9b expression. Further mechanistic studies have demonstrated a direct association of caspase-9b with the cellular inhibitor of apoptosis 1 (cIAP1), a regulatory factor in both arms of the NF-κB network, via its IAP-binding motif. Through this interaction, caspase-9b induces the E3 ligase activity of cIAP1, which regulates NF-κB activation, and promotes the survival, anchorage-independent growth and tumorigenicity of NSCLC cells. Overall, a novel tumorigenic mechanism has been identified, by which alternative mRNA processing regulates the NF-κB signaling independent of external agonist.

CHAPTER 1 – INTRODUCTION:
REGULATION OF CASPASE-9 SPLICING BY HNRNP U

1.1 Non-small cell lung cancer

Lung cancer is the leading cause of cancer-related death in both men and women worldwide and accounts for an estimated 28% of all cancer deaths in the United States (50). Death rates from lung cancer have not been changed considerably over the past 50 years despite the advances in cancer treatment and improvements in lifestyle and health care. Non-small cell lung cancer (NSCLC) represents the majority of lung cancers with poor prognosis and a cumulative five-year survival rate of less than 18% (70). Most patients present with unresectable disease and therefore, chemotherapy and/or radiation are the current treatment options. However, the treatment efficacy is restricted by the rapid development of chemo- or radio-resistance (13). Thus, development of new therapy approaches, especially new therapeutic targets, is necessary to reduce the mortality from this disease.

1.2 Apoptosis: the intrinsic and extrinsic pathway

Apoptosis is a distinctive mode of "programmed cell death", which plays critical roles in regulation of tissue homeostasis (18). Apoptosis process is often energy-dependent, irreversible and highly coordinated by a cascade of molecular events. The most important factor mediating apoptosis is a group of cysteine proteases called caspases, which are capable of cleaving

specific proteins in the cytoplasm and nucleus to trigger cell death. Caspases exist in the cells as inactive precursors, or procaspases, which are usually activated by other caspases, resulting in a proteolytic caspase cascade. Caspase activation is regulated by members of the Bcl-2 family and the inhibitor of apoptosis (IAP) proteins.

Two main apoptotic pathways have been identified: the extrinsic or death receptor pathway and the intrinsic or mitochondrial pathway (figure 1.1). Although these two pathways differ in the initiation phase, they both end at the point of the execution phase including caspase-3 activation, DNA fragmentation, degradation of cytoskeletal and nuclear proteins, protein crosslinking, formation of apoptotic bodies, expression of ligands for phagocytic cell receptors and uptake of apoptotic bodies by phagocytic cells. For the initiation phase in the extrinsic pathway, engagement of death receptors results in the formation of the death-inducing signaling complex (DISC) containing the death receptors, adaptor proteins, caspase-8 and caspase-10 whereas the intrinsic pathway is initiated by the release of cytochrome c from the mitochondria into the cytosol to trigger the formation of apoptosome containing cytochrome c, apaf-1 and caspase-9. Further recruitment of caspases to DISC and apoptosome leads to their activation by dimer formation.

Various key factors in apoptosis have been identified; however, the molecular mechanisms of many of these remain inclusive. Since dysregulation of apoptosis, either increased or inadequate apoptosis, is implicated in many disease states, including neurodegenerative disorder, acquired immune deficiency syndrome (AIDS), ischemic damage, autoimmune disorders and many types of cancer, further studies regarding the mechanisms of apoptosis would have significant impacts on developing therapeutic strategy against apoptosis-related diseases.

1.3 Caspase-9 splicing

Among the 14 caspases identified to date, caspase-9 is one of the most important initiators of the intrinsic apoptotic pathway. For example, the activation of caspase-9 via interaction with Apaf-1 and cytochrome c to form the apoptosome activates downstream caspases to amplify apoptotic signaling. There are two splice variants of caspase-9, caspase-9a and caspase-9b, that can be generated by the inclusion or exclusion of exon 3,4,5,6 cassette in the mature caspase-9 mRNA (figure 1.2). Different from caspase-9a (or procaspase-9), caspase-9b lacks the catalytic domain, but retains the caspase recruitment/Apaf-1 association domain (CARD) (figure 1.2). Thus, apposing to caspase-9a, which is a pro-apoptotic protein, caspase-9b functions as an apoptotic inhibitor by competing with caspase-9a for binding to Apaf-1 and consequently suppressing caspase-cascade activation (55, 59).

The ratio of caspase-9a/9b isoform is dysregulated in NSCLC cells (21, 57), and several factors implicated in regulating the alternative splicing of caspase-9 include endogenous ceramides (8), SRSF1 (SRp30a or ASF/SF2) (45, 57, 58) and heterogeneous nuclear ribonucleoprotein L (hnRNP L) (21). De novo ceramide synthesis and SRSF1 have been documented to down-regulate the level of caspase-9b mRNA in contrast to hnRNP L, which represses the inclusion of four-exon cassette to favor the formation of caspase-9b. Importantly, phosphorylation of SRSF1 or hnRNP L and subsequent effects on the caspase-9 splicing process has been shown to be important in sensitizing non-small cell lung cancer (NSCLC) cells to chemotherapeutics and promoting the tumorigenic capacity of these cells (21, 58). Hence, modulation of caspase-9 splicing or caspase-9 splice variant ratio would be a promising cancer-specific approach for treatment of NSCLC.

1.4 hnRNP U protein

hnRNP U, also known as SP120, is the largest of major heterogeneous nuclear ribonucleoproteins (120 KDa). It is capable of binding to both DNA through the acidic region in the N-terminal and RNA via the RGG box in the C-terminal (19, 34) (figure 1.3). hnRNP U is also a major constituent of nuclear matrix or scaffold and is, thereby, termed scaffold attachment factor A (SAF-A). Various biological functions of hnRNP U have been reported: regulation of gene transcription (17, 35, 36, 53), controlling RNA stability (68), participating in X inactivation process (23, 25) and controlling telomere length (20). The splicing regulatory function of hnRNP U has just emerged recently (69) with hnRNP U shown to modulate SMN2 splicing via controlling U2 snRNP maturation. The multiple biological roles of hnRNP U might explain why mice carrying a hypomorphic mutation in the hnRNP-U gene exhibit post-implantation lethality.

1.5 Specific aims of the study

Previously in the laboratory, four RNA *trans*-factors were identified to associate with the purine-rich sequences in C9/E3, including hnRNP L, hnRNP A2/B1, hnRNP R and hnRNP U (Table 1.1), and this association suggested a possible biological function in regulating caspase-9 mRNA processing (21). The roles of hnRNP L and hnRNP A2/B1 on caspase-9 splicing were further examined by Goehe et al in the laboratory (21). In this study, we examined the roles of the two other factors, hnRNP U and hnRNP R, on caspase-9 RNA splicing and found the involvement of hnRNP U in regulating caspase-9 splicing through interaction with target mRNA. The precise binding sites for hnRNP U on caspase-9 mRNA were also determined. Additionally, we investigated the mechanism that regulates the interaction between hnRNP U and exon 3 of caspase-9, which determines the preferential expression of caspase-9a or caspase-9b.

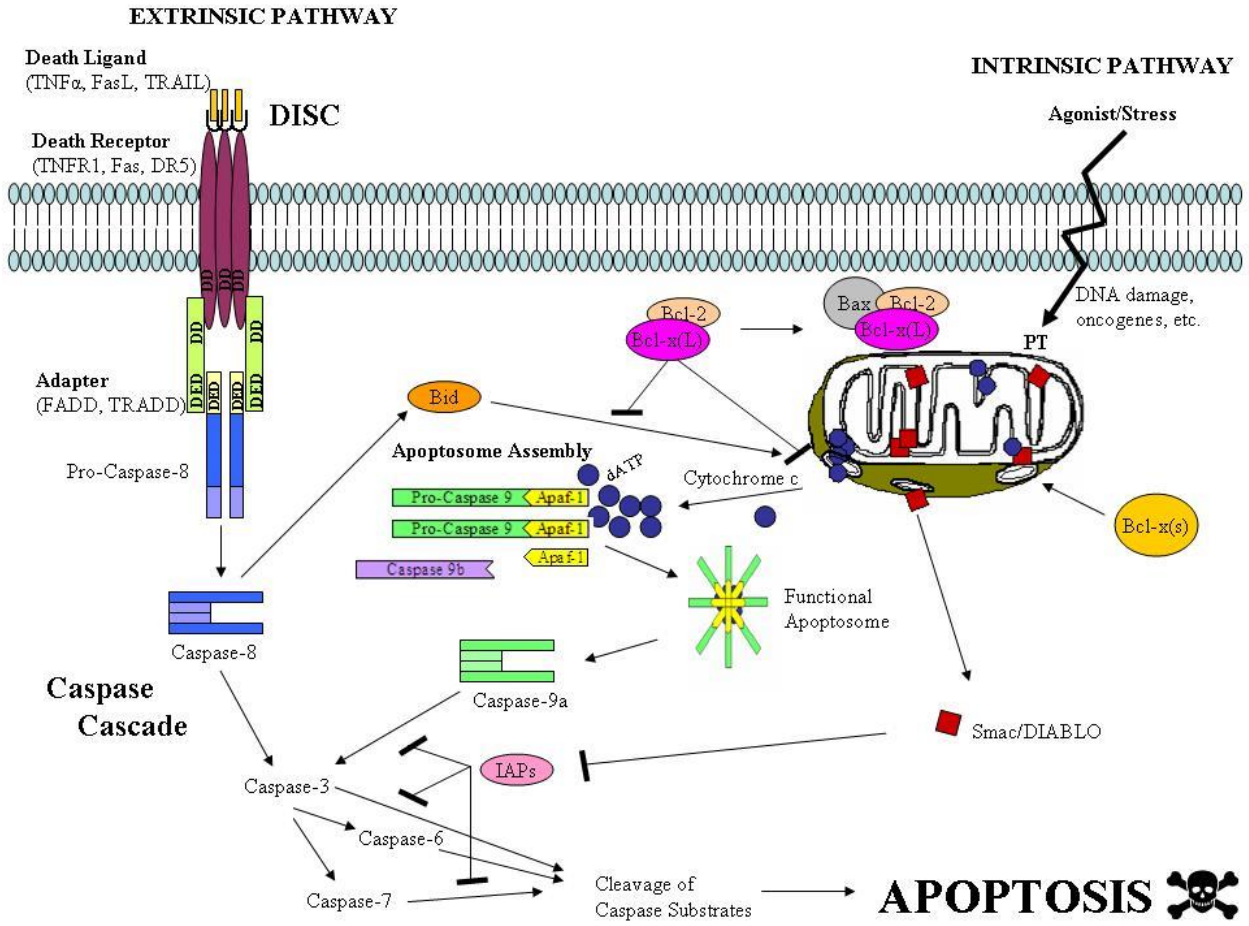

Figure 1.1 Intrinsic and extrinsic pathway in apoptosis. The intrinsic pathway is initiated within the cells and is triggered by different signals as a result of DNA damage, severe cell stress or loss of cell-survival factors. Activation of the intrinsic pathway normally leads to the release of pro-apoptotic proteins from the mitochondria, the center of the intrinsic signaling, to activate caspase cascade, including the initiator and effector caspases, and execute apoptosis. The extrinsic pathway is initiated outside the cell via association between the pro-apoptotic ligands and pro-apoptotic receptors on the cell surface. Ligand binding results in receptor clustering and formation of death-inducing signaling complex (DISC). After DISC activation, the extrinsic pathway utilizes the same effector caspase machinery as the intrinsic pathway.

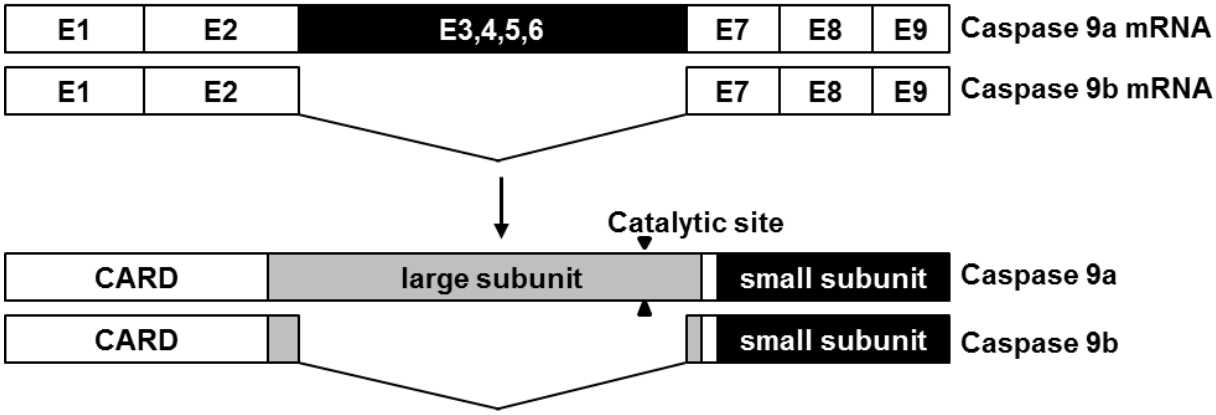

Figure 1.2 Schematic representation of caspase-9a/b mRNA and protein structure. The alternative splicing of caspase-9, specifically the inclusion or exclusion of the four-exon cassette, generates two different splicing products, caspase-9a and caspase-9a. Caspase-9b protein translated from caspase-9b splice variant lacks almost the large subunit, including the catalytic site.

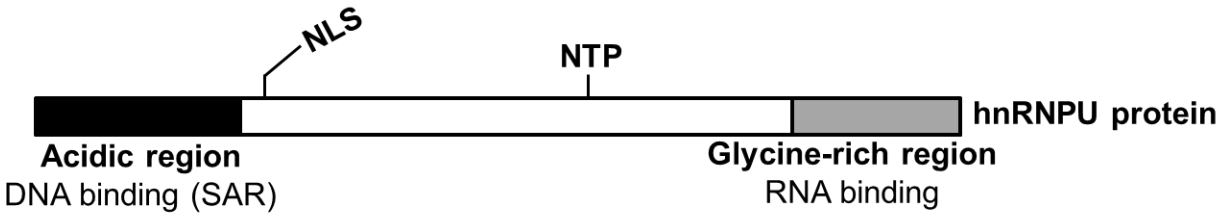

Figure 1.3 Schematic representation of hnRNP U protein structure. hnRNP U contains the amino-terminal acidic region, which mediates its binding to DNA sequence termed scaffold attachment region (SAR), and RGG box in the carboxy-terminal glycine-rich region, which enables it to bind to RNA sequence. NLS and NTP denotes the putative nuclear localization signal and NTP binding site.

CHAPTER 2 – MATERIALS AND METHODS: REGULATION OF CASPASE-9 SPLICING BY HNRNP U

2.1 Cell culture

A549 lung adenocarcinoma cells were cultured in DMEM medium with 10% (v/v) FBS (Sigma-Aldrich), 100 U/ml penicillin and 100 µg/ml streptomycin sulfate (Invitrogen). Human bronchial epithelial primary cells (HBEpC) were cultured in Bronchial/Tracheal Epithelial Cell Growth medium (Cell Applications). All cells were maintained at less than 80% confluency under standard incubator conditions. For the comparison studies between A549 versus HBEpC cell lines, cells were plated in tissue culture plates (100 mm), which gave 40% confluency. The following day, medium was changed to serum-free DMEM and cell plates were incubated overnight before total protein or cell lysates were isolated for analysis.

2.2 Electrophoretic mobility shift assay (EMSA)

RNA-binding reaction mixtures (20 µl) containing 10 µg of A549 or HBEpC cell lysates, 40 U RNASIN, 11.3 µg tRNAs, 10 mM HEPES, 5 mM DTT, 120 mM KCl, 3 mM $MgCl_2$, 5% glycerol and 10 µM of FITC tagged RNA oligos (C9/E3 WT, C9/E3 Mut1, C9/E3 Mut2, C9/E3 Mut3 or C9/E3 Mut4) were incubated on ice for 20 minutes. Then 2 µg of hnRNP U antibody or BSA (control) was added to each binding mixture and the mixtures were incubated for additional 30 minutes. Samples were loaded on a 5% TBE-polyacrylamide gel for electrophoresis separation. RNA-protein complexes were then visualized by using Molecular Imager FX (Bio-Rad) with a 488 nm EX (530 nm BYPASS) laser.

2.3 Densitometric analysis of the EMSA supershift

The fold-differences in hnRNP U-E3/C9 binding between A549 and HBEpC cells were determined by densitometric measurement of the hnRNP U supershift in the scanned EMSA gels from three independent experiments (n=4) using ImageJ densitometry software (NIH).

2.4 Mass spectrometry analysis

Analysis of RNA-protein complexes was performed at the Emory University Mass Spectrometry Center (Atlanta, Georgia, USA) as previously described (21). Briefly, RNA-protein complexes retrieved from EMSA were excised from the gel following by in-gel trysin digestion. The tryptic mixtures were then analyzed by nano– LC-MS/MS. Nano–LC-MS/MS results were obtained by searching through Mascot database (Matrix Science).

2.5 siRNA transfection

A549 or HBEpC cells were transfected with negative control siRNA or hnRNP U SMARTpool siRNA or hnRNP R siRNA (Dharmacon) using Dharmafect 1 transfection reagent (Dharmacon). Cells (3-4 x 10^5) were plated in each well of 6-well tissue culture dishes in regular growth medium. The following day, cells were plated in Opti-MEM I medium without antibiotics/FBS and transfected with 100 nM of siRNA (diluted in 1X siRNA buffer). After 4 hours of incubation, 0.5 ml Opti-MEM I medium containing 3-fold the normal concentration of antibiotics/FBS was added to the 1ml of transfection mixture. Cells in transfection mixture were incubated for additional 4 hours before medium was changed to normal growth medium. After 48 hours, total RNA or protein was collected from the cell lysates.

2.6 Competitive RT-PCR

Total RNA was extracted from the cells using the RNeasy Mini Kit (Invitrogen) and then reverse transcribed to cDNA using SuperScript III Reverse Transcriptase Kit (Invitrogen). The

reverse transcription reaction products were utilized in PCR for the endogenous caspase-9 primers (sense primer 5'-CATGCTGGCTTCGTTTCTG-3' and anti-sense primer 5'-AGGGGCAAACAACAGATGG-3'). PCR was performed in 25 cycles of 94^{o}C for 30 seconds, 58^{o}C for 30 seconds and 72^{o}C for 1 minute. The final PCR products were resolved on 5% TBE polyacrylamide gel, stained with SYBR Gold (Invitrogen) and visualized by using Molecular Imager FX (Bio-Rad) with a 488 nm EX (530 nm BYPASS) laser.

2.7 Quantitative RT-PCR

Total RNA was extracted from the cells using the RNeasy Mini Kit (Invitrogen) and then reverse transcribed to cDNA using SuperScript III Reverse Transcriptase Kit (Invitrogen). The reverse transcription reaction products were utilized for real-time PCR for Casp9a, Casp9b, and 18s using TaqMan PCR master mix and the Applied Biosystems 7500 Real-Time PCR System. Casp9a and 18s q-PCR primers were ID numbers Hs00154261_m1 and Hs99999901_s1. The q-PCR primers for Casp9b were 5'-GGATTTGGTGATGTCGAGCAG-3′ (forward), 5′-CATCTGGCTCGGGGTTACT-3′ (reverse) and 5′-TTCCCCTGAAGACGAGTCCCCTGG-3′ (probe). The relative amount of Casp9a or Casp9b was normalized to 18s.

2.8 Cell lysate preparation

Cell lysates, except for the CIP experiments, were prepared by lysing the cells in NP-40 lysis buffer (50 mM Tris-HCl at pH 8.0, 150 mM NaCl, 1% NP-40 and 1X protease/protein phosphatase inhibitor cocktail). For cell lysates utilized for the CIP treatment experiments, cells were lysed in the same NP-40 buffer as detailed above, but without protein phosphatase inhibitors. Lysates were also utilized "fresh" for these experiments (i.e. same day), and not stored.

2.9 Streptavidin-biotin affinity purification (SBAP)

Reaction mixtures (20 µl) containing 10 µg of cell lysates or 4 µg of IgG (control), 40 U RNASIN, 11.3 µg tRNAs, 10 mM HEPES, 5 mM DTT, 120 mM KCl, 3 mM $MgCl_2$, 5% glycerol and 10 µM biotinylated RNA oligo (C9/E3 WT, C9/E3 Mut1, C9/E3 Mut2, C9/E3 Mut3 or C9/E3 Mut4) were incubated on ice for 30 minutes. Pre-washed streptavidin-agarose beads were then added to the reactions following by 2 hour of incubation with gentle agitation (4°C). After incubation, the reactions were washed 3 times with pre-block buffer (100 mM KCl, 20 mM Tris-HCl at pH 7.5 and 0.2 mM EDTA) and centrifuged to collect the pellet. The pellet was resuspended in Laemmli buffer, dry-boiled for 10 minutes and subjected to western immunoblotting.

2.10 *In vitro* phosphatase treatment

Phosphatase reaction mixtures containing 10 µg cell lysate and 10U calf-intestinal phosphatase (CIP) or heat-inactivated CIP (denatured CIP, control) in 1X NEBuffer 3 (New England BioLabs) were incubated at 37^{o}C. After 1 hour of incubation, 1X phosphatase inhibitor cocktail was added to the mixtures. Reaction mixtures were then utilized in EMSA or SBAP for RNA-protein binding analysis.

2.11 Immunoprecipitation (IP)

Cells were lysed in 1X IP buffer containing 1% Trition X-100, 150 mM NaCl, 10 mM Tris pH 7.4, 1mM EDTA pH 8.0, 0.5% NP-40 and 1X phosphatase/protease inhibitor cocktail. Sample lysates (200 µg) were pre-cleared with pre-washed protein G Sepharose beads for 1 hour at 4^{o}C in gentle agitating condition. After pre-clearing, samples were centrifuged and collected from the supernatants. 4 µg of hnRNP U or hnRNP L monoclonal antibody was placed in each sample and in 4^{o}C for 2 hour with gentle agitation before pre-washed protein G Sepharose beads

were added. The following day, the bead complexes were centrifuged, washed extensively with 1X IP buffer, pelleted by centrifugation, resuspended in Laemmli buffer, dry-boiled for 10 minutes and subjected to SDS-PAGE/immunoblotting. For IP experiments coupled with CIP treatment, cells were lysed in the same IP buffer, but without protein phosphatase inhibitors. The IPs were then subjected to CIP treatments as detailed in the above method section.

2.12 *In vitro* kinase assay

Kinase reaction mixtures (20 µl) containing 80 ng of recombinant hnRNP L, 10 mM HEPES, 5 mM DTT, 120 mM KCl, 3 mM $MgCl_2$, 5% glycerol, 0.5 mM ATP, 1.25 mM glycerol-2-phosphate and 200 ng of AKT2 (Sigma) were incubated at 30^{o}C for 30 minutes. Reaction mixtures were then utilized in EMSAs for RNA-protein binding analysis or SBAP-based competitive binding assays.

2.13 Competitive binding assay

Recombinant hnRNP L was subjected to *in vitro* kinase assay. Kinase reaction mixtures (20 µl) were then incubated with 40 U RNASIN, 11.3 µg tRNAs, 10 mM HEPES, 5 mM DTT, 120 mM KCl, 3 mM $MgCl_2$, 5% glycerol and 10 µM biotinylated C9/E3 ROs on ice for 30 minutes. Pre-washed streptavidin-agarose beads were then added to the reactions following by 2 hour of incubation with gentle agitation (4°C). After incubation, the reactions were washed 3 times with pre-block buffer (100 mM KCl, 20 mM Tris-HCl at pH 7.5 and 0.2 mM EDTA) and centrifuged to pellet the bead complexes. The bead complexes were then incubated with binding mixtures (20 µl) containing 10 µg of HBEpC cell lysates, 40 U RNASIN, 11.3 µg tRNAs, 10 mM HEPES, 5 mM DTT, 120 mM KCl, 3 mM MgCl and 5% glycerol for additional 2 hours. After incubation, the bead complexes were washed 3 times with pre-block buffer (100 mM KCl, 20

mM Tris-HCl at pH 7.5 and 0.2 mM EDTA), pelleted by centrifugation, resuspended in Laemmli buffer, dry-boiled for 10 minutes and subjected to SDS-PAGE/immunoblotting.

2.14 Statistical analysis

Statistical differences in the mRNA level between the control and hnRNP U siRNA treated cells were determined by a 2-tailed, unpaired Student's *t* test. Statistical differences in the association of hnRNP U with E3/C9 between A549 and HBEpC cells were determined by one-sample *t*-test. *P* values of less than or equal to 0.05 were considered significant.

2.15 Antibody information

The following antibodies were used in western immunoblotting or EMSA/supershift: anti-caspase-9 (Assay Designs), anti-hnRNP U (Sigma-Aldrich), anti-β-actin (Cell Signaling Technology), anti-laminA/C (Cell Signaling Technology), anti-phospho-serine (Cell Signaling Technology), anti-phospho-threonine (Cell Signaling Technology), anti-phospho-(serine/threonine)-AKT substrate (Cell Signaling Technology), AKT2 (Cell Signaling Technology), anti-hnRNP L (Santa Cruz Biotechnologies Inc.), anti-phospho-Ser52-hnRNP L (custom anti-produced via Genscript Corporation) (21), horseradish peroxidase-conjugated anti-rabbit IgG antibody (Cell Signaling Technology) and horseradish peroxidase-conjugated anti-mouse IgG antibody (Cell Signaling Technology).

CHAPTER 3 – RESULTS:
REGULATION OF CASPASE-9 SPLICING BY HNRNP U

3.1 Identification of hnRNP U associated with exon 3 of caspase-9 and suppressing the formation of the caspase-9b isoform

Using EMSA coupled to nanospray LC-MS/MS analysis, four RNA *trans*-factors, hnRNP L, hnRNP A2/B1, hnRNP R and hnRNP U, were previously identified to associate with the purine-rich sequences in C9/E3 (Table 1.1) (21). hnRNP L was then further characterized to modulate the alternative splicing of caspase-9 pre-mRNA as a repressor of the inclusion of the exon 3,4,5,6 cassette whereas hnRNP A2/B1 did not affect caspase-9 splicing (21). Here, we examine the roles of the two other RNA *trans*-factors, hnRNP U and hnRNP R, on the alternative splicing of caspase-9 by employing siRNA technology. Whereas downregulation of hnRNP U reduced the endogenous caspase-9a/9b mRNA ratio in both transformed A549 cells and non-transformed human bronchial epithelial primary cells (HBEpC) (Fig. 1.4A-D), hnRNP R depletion yielded no change in the ratio of caspase-9a/9b mRNA (Fig. 1.4A and B). Importantly, the effect of hnRNP U on the mRNA ratio translated to the protein level (Fig. 1.4E). These data indicate that hnRNP U inhibits the formation of caspase-9b via suppressing the exclusion of four-exon cassette in the mature caspase-9 mRNA.

Since the two splice variants of caspase-9, caspase-9a and caspase-9b, are generated from the same gene and have the same 5'UTR and 3'UTR sequences, the effect of hnRNP U depletion on caspase-9a/9b ratio is likely attributable to the regulation of the alternative splicing of caspase-9 rather than mRNA stability. Indeed, no significant difference in the decay rate (specifically, RNA half-life $t_{1/2}$) of caspase-9a or caspase-9b mRNA was observed after treatment of the control versus hnRNP U-depleted cells with actinomycin D (Fig. 1.4F-H). These data "rule out" the possibility that hnRNP U represses the production of caspase-9b by stabilizing caspase-9a mRNA or destabilizing caspase-9b mRNA. Hence, regulation of the alternative splicing of caspase-9 is most likely the mechanism contributing to the observed enhancing function of hnRNP U in the inclusion of the four-exon cassette.

3.2 hnRNP U binds specifically to exon 3 of caspase-9 pre-mRNA

The LC-MS/MS results strongly suggested that hnRNP U interacted with C9/E3. To determine whether hnRNP U interacts specifically with C9/E3, EMSA coupled with an hnRNP U "supershift" was performed (Fig. 1.5A and Table 1.2 for sequences utilized). Indeed, a "supershift" was observed after the addition of an anti-hnRNP U antibody indicating that hnRNP U is present in the C9/E3-protein complex, and thereby, verifying the LC-MS/MS results (Fig. 1.5B). Furthermore, this "supershift" was specific for hnRNP U since reduction in levels of hnRNP U via siRNA resulted in the loss of the supershift (Fig. 1.5C and D).

Mutagenesis analysis was employed to further determine/validate the binding site for hnRNP U in C9/E3. As shown in Fig. 1.5E and F, the interaction between hnRNP U and C9/E3 was completely abolished in one out of four C9/E3 mutations (Mut3). Interestingly, this interaction site has been previously identified as the binding site for hnRNP L, a repressor that regulates the alternative splicing of caspase-9 (21). Two additional mutations (Mut2 and Mut4) flanking this

site also significantly diminished the association of hnRNP U to C9/E3 (Fig. 1.5E and F). These findings reveal that hnRNP U specifically interacts with the hnRNP L binding site in C9/E3. Also of note, almost a complete loss of protein:RNA complexes was observed with Mut3 in accord with our previous findings of hnRNP L binding to this region. These data also suggest that hnRNP L, hnRNP U, or both may also target additional RNA *trans*-factors to exon 3 of caspase- 9.

3.3 Phosphorylation regulates the interaction between hnRNP U and exon 3 of caspase-9 pre-mRNA

Although hnRNP U was expressed at the same level in non-transformed (HBEpC) versus transformed (A549) cells (Fig. 1.6A), the association of this RNA *trans*-factor to C9/E3 in HBEpC cells was significantly higher than in A549 cells (Fig. 1.6B and C). Specifically, the fold-difference as assayed by EMSA analysis was 1.70 ± 0.18 (mean ± SD) ($p < 0.01$).

Selective phosphorylation of hnRNP U has been reported in a study of Burglund and Larke (2009) (3). Thus, we hypothesized that the enhanced binding of hnRNP U to C9/E3 in non-transformed cells compared to transformed cells was due to the differences in post-translational modification, particularly the phosphorylation state. To address this possibility, protein phosphatase treatments coupled with RNA binding assays were undertaken. Congruent with our hypothesis, the dephosphorylation of NSCLC (A549) cell lysates resulted in significant enhancement of the association of hnRNP U to C9/E3 (Fig. 1.6C-E). These findings implicate phosphorylation as a regulatory mechanism for hnRNP U-C9/E3 interaction, which may explain the differences observed in non-transformed versus transformed cells regarding hnRNP U-C9/E3 binding.

To determine whether the phosphorylation of RNA *trans*-factors was the mitigating factor in modulating the differential association of hnRNP U to C9/E3 in transformed cells versus non-transformed cells, both A549 and HBEpC cell lysates were subjected to phosphatase (CIP) treatment (denatured versus active) in the absence of protein phosphatase inhibitors. Dephosphorylation of A549 cell lysates increased the association of hnRNP U to C9/E3 to comparable levels of the binding observed in HBEpC cell lysates, whereas the association of hnRNP U in the non-transformed cells was unaffected (Fig. 1.6F). These data demonstrated that the disparity in hnRNP U binding between transformed and non-transformed cells is due to the phosphorylation state of RNA *trans*-factors (Fig. 1.6G).

3.4 Inhibition of the AKT pathway promotes the association of hnRNP U with C9/E3 and alters the ratio of caspase-9 splice variants

The phosphoinositide 3-Kinase/AKT pathway has been reported to modulate the alternative splicing of caspase-9 (57), and we hypothesized that this signaling pathway modulates the ability of hnRNP U to bind C9/E3. Indeed, treatment the NSCLC cells with AKT1/2 inhibitor increased the binding of hnRNP U to C9/E3 in a dose-responsive manner, but did not significantly affect its expression level (Fig. 1.7A). Importantly, enhanced association of hnRNP U to C9/E3 by AKT inhibitor treatment correlated with the increasing caspase-9a/9b ratio in NSCLC cells (Fig. 1.7A). In contrast, ectopic expression of constitutively active AKT2 (caAKT2) in non-transformed HBEpC cells attenuated the binding of hnRNP U to C9/E3, which correlated with a decrease in the caspase-9a/9b ratio (Fig. 1.7B). These data demonstrate that AKT signaling regulates the interaction of hnRNP U with caspase-9 pre-mRNA.

3.5 The phospho-state of hnRNP U is not affected by AKT inhibition

The culmination of our data coupled to reports in the literature of hnRNP U being selectively phosphorylated led to the initial hypothesis that the phospho-state of hnRNP U regulates the association of the RNA *trans*-factor to C9/E3 (Fig. 1.7G). In direct opposition to this hypothesis, treatment of A549 cells with an AKT inhibitor had no significant effect on the phosphorylation state of hnRNP U (Fig. 1.8A) and *in vitro* phosphatase treatment showed a minor effect on serine-phosphorylation (Fig. 1.8B). Importantly, treatment with AKT inhibitor or phosphatase in the same condition has been shown to affect the binding of hnRNP U to C9/E3 (figure 1.6D, E, F and figure 1.7A), which indicates that phospho-state of hnRNP U does not play an important role in regulating the association of the RNA *trans*-factor with C9/E3.

3.6 hnRNP L is phosphorylated in an AKT-dependent manner inducing competition with hnRNP U for C9/E3 binding

Since the phospho-state of hnRNP U is not critical to hnRNP U-C9/E3 interaction, we hypothesized that the phosphorylation of other regulatory RNA *trans*-factors modulated the ability of hnRNP U to associate with C9/E3. In this regard, hnRNP U shares the same binding site as hnRNP L, which has the opposite function in regards to regulating the alternative splicing of caspase-9 pre-mRNA. Therefore, we examined the direct binding of recombinant hnRNP L purified from non-transformed HEK293 cells to the C9/E3. Interestingly, direct binding of recombinant hnRNP L to this purine-rich sequence was not observed by EMSA (Fig. 1.9A, lane 1), congruent with a report showing the interaction of this recombinant hnRNP L to be specific for CA-repeats (51). As caspase-9 RNA splicing is regulated by the phosphorylation of hnRNP L (21), we examined whether AKT directly phosphorylates hnRNP L and induces the association of the RNA *trans*-factor with C9/E3. Intriguingly, AKT efficiently phosphorylated hnRNP L,

which induced its binding to C9/E3 (Fig. 1.9A). Moreover, inhibition of AKT signaling in NSCLC cells directly by AKT inhibitor treatment or indirectly by blocking EGFR activity with erlotinib treatment significantly reduced the phospho-state of hnRNP L (Fig. 1.9B). Lastly, hnRNP L phosphorylated by AKT interfered with hnRNP U for binding to C9/E3 (Fig. 1.9C) in contrast to non-phosphorylated hnRNP L. Taken together, these data demonstrate that the phospho-status of hnRNP L is regulated by AKT signaling in NSCLC, which induces the association of this RNA *trans*-factor and restricts the access of the enhancing factor, hnRNP U, to C9/E3 (Fig. 1.9D).

Table 1.1 RNA *trans*-factors associated with exon 3 of caspase-9 in NSCLC cells.

RNA *trans*-factors
hnRNP A2/B1
hnRNP L
hnRNP R
hnRNP U

Table 1.2 RNA oligos (ROs) utilized in the RNA binding assays (EMSA or SBAP). For mutant C9/E3 ROs, the mutated sites are located in the underlined sequences.

RO code	**Sequence**
NSC	CAGAAUUCGCACGUUACU
C9/E3 WT	GAGAGUUUGAGGGGAAAU
C9/E3 Mut1	CAGAAUUUGAGGGGAAAU
C9/E3 Mut2	GAGAGCCCGAGGGGAAAU
C9/E3 Mut3	GAGAGUUUCUACUGAAAU
C9/E3 Mut4	GAGAGUUUGAGGGUUACU

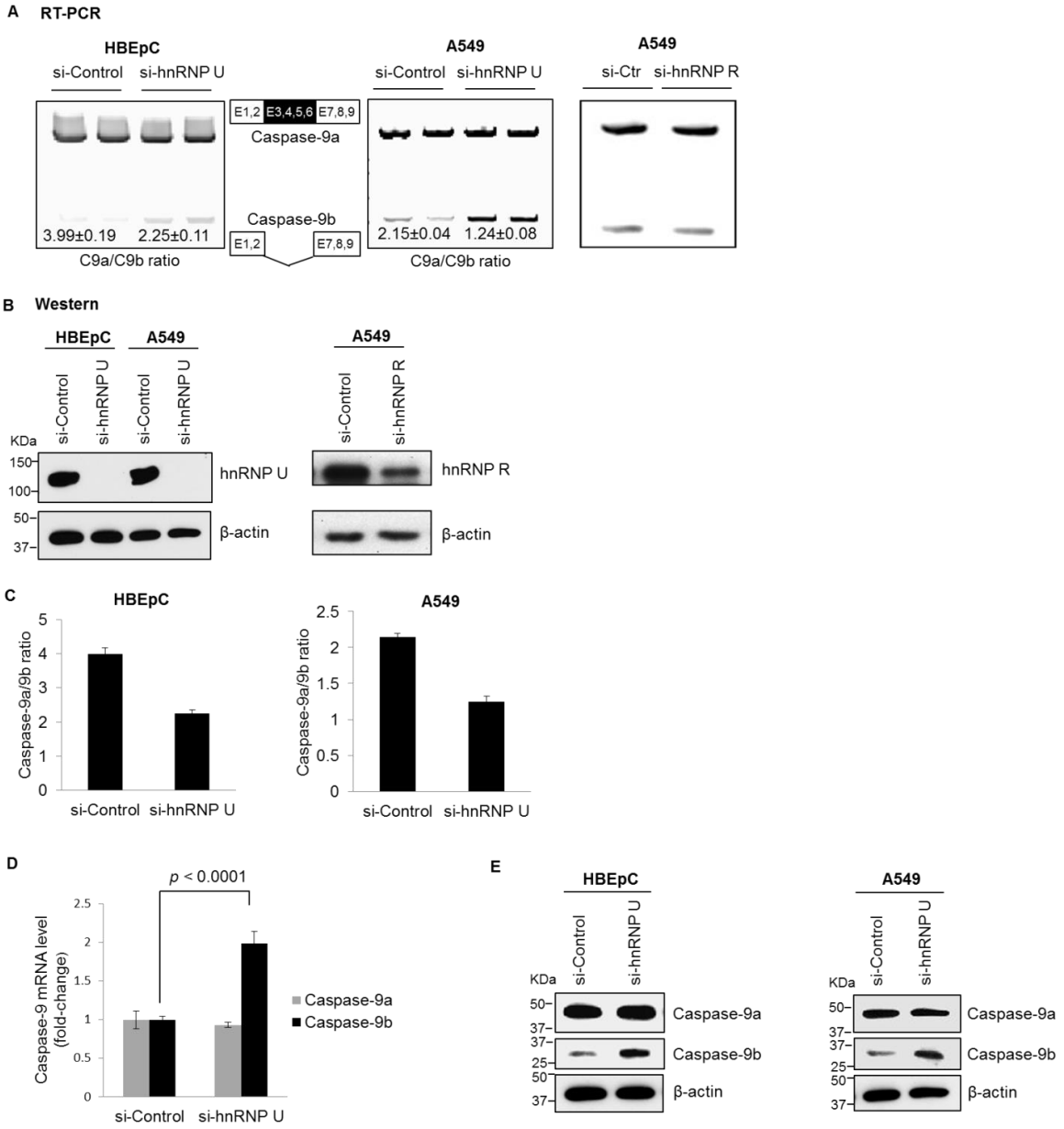

Figure 1.4 hnRNP U, but not hnRNP R, represses the formation of caspase-9b via RNA splicing. A549 or HBEpC cells were transfected with control siRNA (100 nM), hnRNP U SMARTpool siRNA (100 nM), or hnRNP R siRNA (100 nM) for 48 hours. (**A**) Total RNA was isolated and analyzed by competitive/quantitative RT-PCR for caspase-9 splice variant ratio using ratio-based quantitation. (**B**) Total protein extracts were subjected to SDS/PAGE/immunoblotting for hnRNP U, hnRNP R or β-actin. (**C**) Graphs were created from the results in (A). (**D**) Total RNA isolated from A549 cells transfected with control or hnRNP U siRNA was analyzed for relative amount of caspase-9a or 9b mRNA by quantitative RT-PCR using the standard curve method and 18s rRNA as a normalizing control. (**E**) Total protein extracts were subjected to SDS/PAGE/immunoblotting for caspase-9 or β-actin. Data are shown as means ± SD (n≥4 on at least 2 independent occasions).

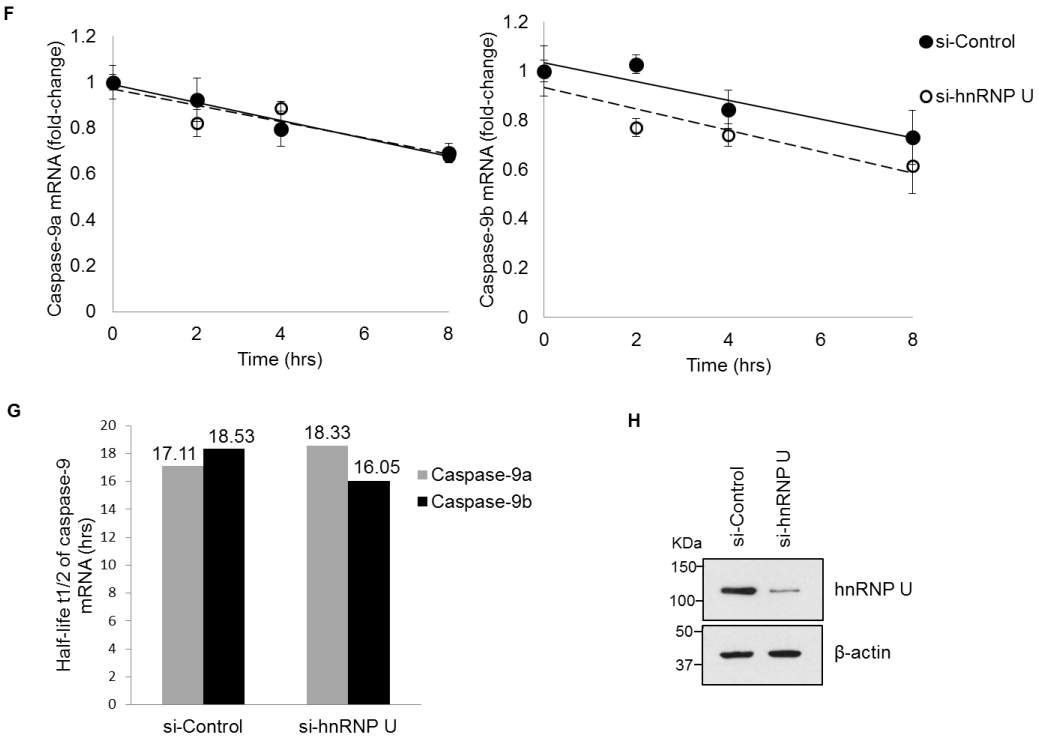

Figure 1.4 (**F**) A549 cells were transfected with siRNA as in (**A**). After 48 hours, cells were treated with actinomycin D (5 μg/ml) for 0, 2, 4 or 8 hours. RNA was isolated and relative amount of caspase-9a or 9b mRNA (fold change compared to the si-control or si-hnRNP U samples at 0 hour) was individually determined by quantitative RT-PCR. (**G**) Half-life of caspase-9a or caspase-9b mRNA was calculated based on the data in (F). (**H**) Total protein from siRNA transfected cells (48 hours) was subjected to SDS/PAGE/immunoblotting for hnRNP U or β-actin. Statistical significance was evaluated by Student's *t* test ($p < 0.0001$, $n = 5$ on two independent occasions).

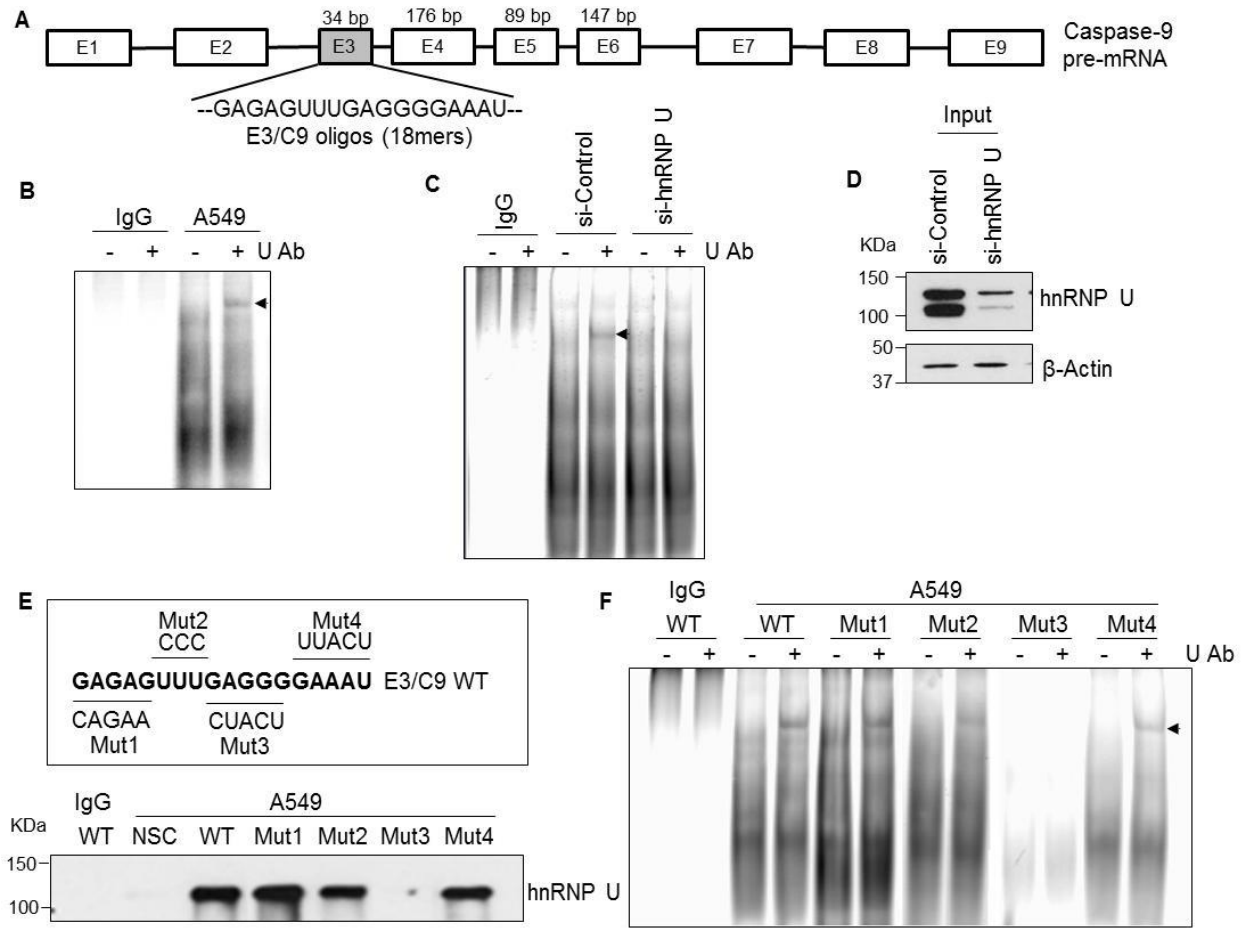

Figure 1.5 hnRNP U binds to exon 3 of caspase-9. (**A**) Schemetic illustration of caspase-9 pre-mRNA structure. 18-mer C9/E3 RNA oligos (ROs) used in RNA binding assays are corresponding to the purine-rich sequence in C9/E3. (**B** and **C**) EMSAs were performed in the absence of protein phosphatase inhibitors using 5'-FITC tagged C9/E3 ROs and in the presence of IgG (control), A549 cell lysates (B) or lysates from A549 cells transfected with control siRNA or hnRNP U SMARTpool siRNA (C). (**D**) Cell lysate input in (C) was subjected to SDS-PAGE and immunoblotted for hnRNP U and β-actin. (**E**) SBAP was performed using 5'-biotinylated non-specific control (NSC), 5'-biotinylated wild-type C9/E3 ROs (C9/E3 WT) or 5'-biotinylated mutant C9/E3 ROs (C9/E3 Mut1-4) in the presence of IgG (control) or A549 cell lysates. (**F**) EMSAs were performed as in (C), but using addtitional ROs (5'-FITC tagged C9/E3 Mut1-4). Arrows indicate the supershifts obtained by the addition of the hnRNP U antibody. The graphs shown in (B), (C), (E) and (F) are representative of n=4 from three independent experiments.

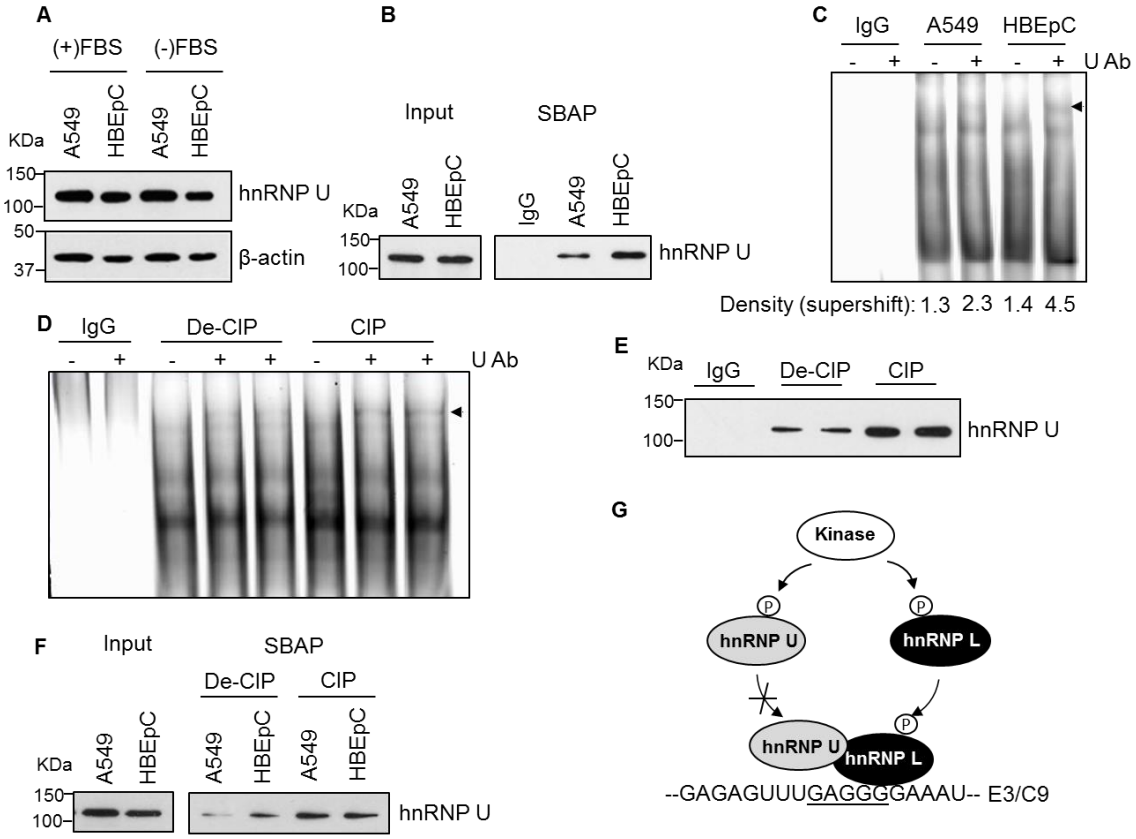

Figure 1.6 Phosphorylation regulates the association of hnRNP U with exon 3 of caspase-9. (**A**) hnRNP U is expressed at the same level in both transformed and non-transformed cells. A549 (transformed) and HBEpC (non-transformed) cells were cultured under the same condition (DMEM media with/without FBS) and confluency. Total protein extracts were subjected to SDS-PAGE/immunoblotting for hnRNP U and β-actin. (**B** and **C**) hnRNP U binds to C9/E3 in higher amounts in HBEpCs than in A549 cells. SBAP assays (B) or EMSAs in the presence of protein phosphatase inhibitors (C) were performed with either IgG (control) or lysates from A549 or HBEpC cells using a 5'-biotinylated or 5-FITC tagged wild-type C9/E3 ROs. (**D** and **E**) Dephosphorylation increases the binding affinity of hnRNP U to C9/E3. A549 cell lysates ("fresh") were pre-incubated with denatured calf-intestinal alkaline phosphatase (de-CIP) or active protein phosphatase (CIP) followed by EMSA (D) in the absence of protein phosphatase inhibitors or SBAP (E) to assay the binding with 5'-FITC tagged (D) or 5'-biotinylated (E) C9/E3 ROs. IgG was used as a control. (**F**) Dephosphorylation abolishes the difference between A549 versus HBEpC regarding the binding of hnRNP U to E3/C9. A549 (transformed) and HBEpC (non-transformed) cells were cultured under the same conditions and confluency, and cell lysates were produced. Lysates ("fresh") were again treated and assayed as in (E). (**G**) Hypothetical model for regulation of hnRNP U/L-C9/E3 interaction by phosphorylation. Whereas the phosphorylation event augments the association between hnRNP L and C9/E3, phosphorylation of hnRNP U attenuates its binding to C9/E3. The graphs shown in (A), (B), (C), (D), (E) and (F) are representative of n=4 from three independent experiments.

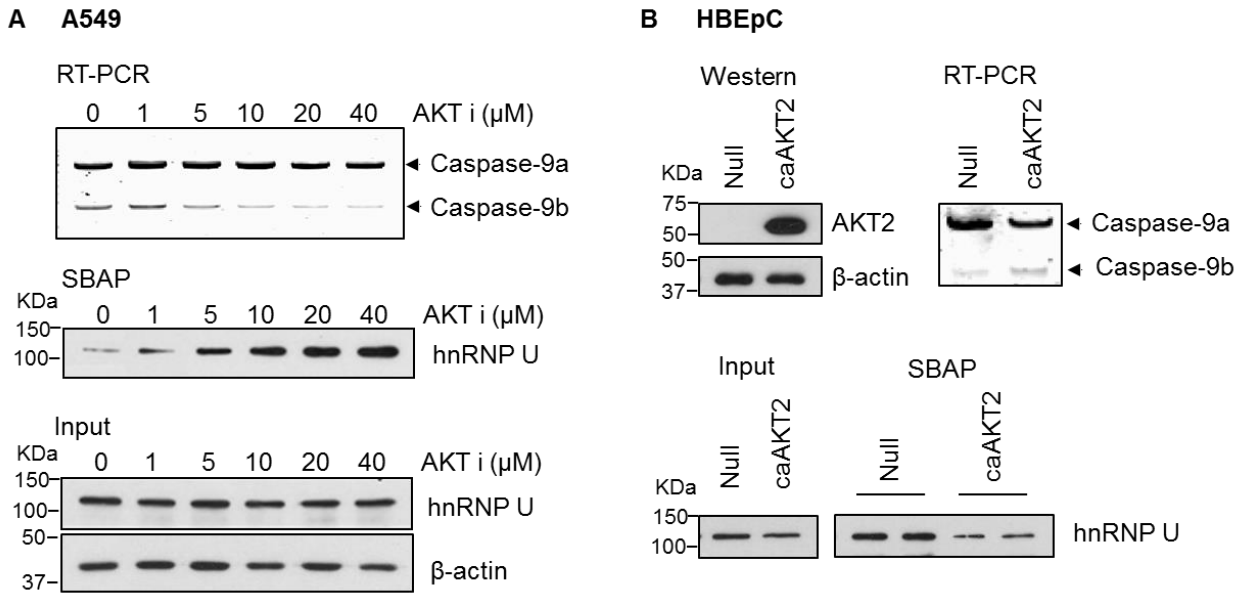

Figure 1.7 AKT pathway regulates the association of hnRNP U to exon 3 of caspase-9. (**A**) Inhibition of AKT1/2 activity increases the caspase-9a/9b ratio and enhances the binding of hnRNP U to C9/E3 in a dose-response manner. A549 cells were treated with 0.1% DMSO control or increasing concentrations of the AKT1/2 inhibitor (AKT VIII). Total RNA was isolated and analyzed for caspase-9 splice variants by competitive/quantitative RT-PCR. Cell lysates from a concomitant experiment were utilized in SBAP to assay the binding of hnRNP U to 5'-biotinylated C9/E3 ROs. Cell lysate input for the SBAP was subjected to SDS-PAGE and immunoblotted for hnRNP U and β-actin. **(B)** Overexpression of AKT decreases both caspase-9a/9b ratio and hnRNP U-E3/C9 association. HBEpC cells were transfected with the control adenovirus or the adenovirus expressing constitutive active AKT2 (caAKT2, 25 MOI) for 48 hours. Total protein or RNA extracts from the transfected cells were then subjected to SDS-PAGE/immunoblotting or competitive/quantitative RT-PCR. Cell lysates were also generated for SBAP to assay the binding of hnRNP U to E3/C9 ROs. The graphs shown in (A) and (B) are representative of n=4 from three independent experiments.

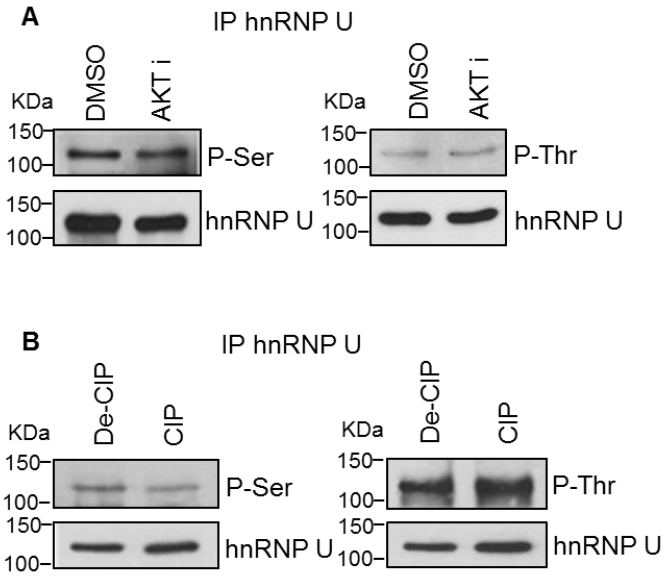

Figure 1.8 AKT inhibition does not alter the phospho-state of hnRNP U. (A) A549 cells were treated with 0.1% DMSO control or AKT1/2 inhibitor (20 µM). Endogenous hnRNP U was then immunoprecipitated (IP) and resolved by SDS-PAGE/ immunoblotting for phospho-serine/threonine or hnRNP U. **(B)** A549 protein extracts were incubated with denatured or active CIP. Endogenous hnRNP U in the resulted protein extracts were immunoprecipitated (IP) and resolved by SDS-PAGE/ immunoblotting for phospho-serine/threonine or hnRNP U. The graphs shown in (A) and (B) are representative of n=3 from two independent experiments.

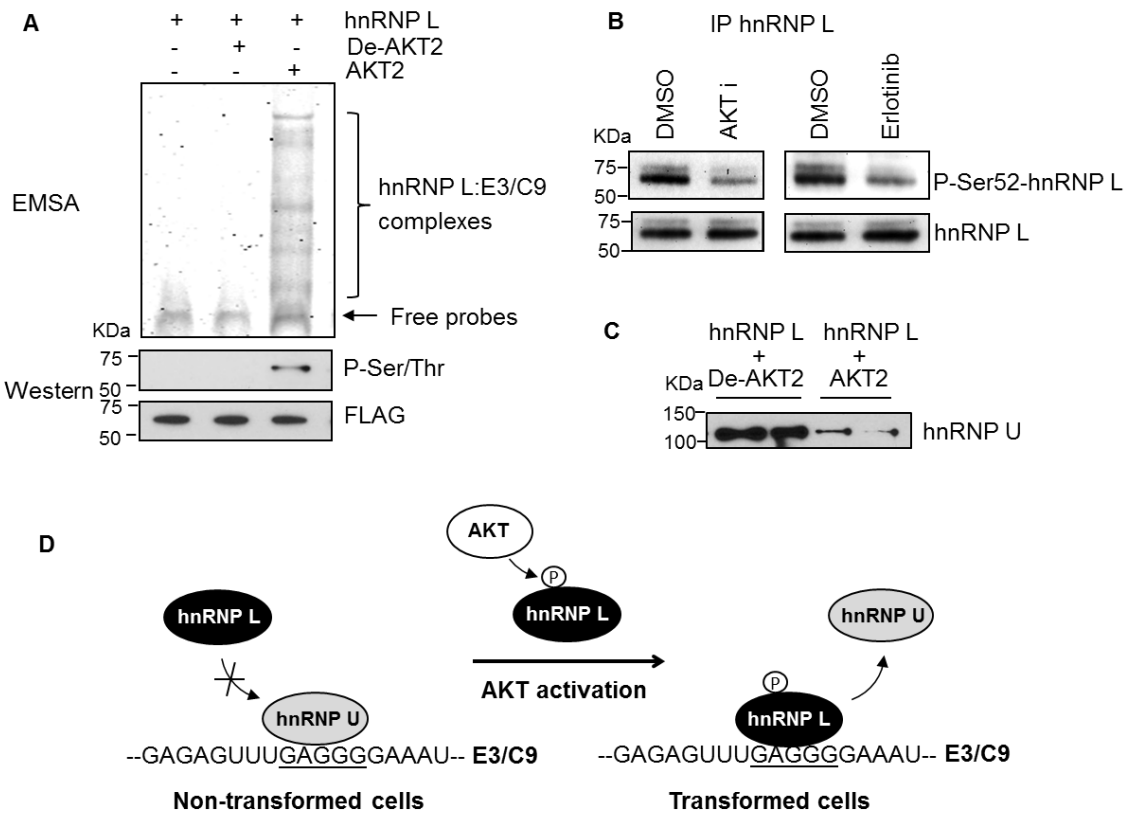

Figure 1.9 AKT-dependent phosphorylation of hnRNP L leads to the competition with hnRNP U for C9/E3 binding. (A) Phosphorylation of hnRNP L by AKT enhances binding to E3/C9. Recombinant FLAG-tagged hnRNP L was phosphorylated *in vitro* using active AKT2 (denatured AKT2 was utilized as a negative control). Products from the kinase assay were then subjected to SDS-PAGE/immunoblotting for phospho-serine/threonine, or the FLAG tag and also utilized in the EMSA to examine the interaction with E3/C9 ROs. (**B**) AKT or EGFR inhibition in NSCLC cells induces a reduction in the phospho-status of hnRNP L. A549 cells were treated with either 0.1% DMSO control, AKT inhibitor (20 μM) or erlotinib (EGFR inhibitor, 1 μM). Endogenous hnRNP L was immunoprecipitated (IP) from the protein extracts. IPed hnRNP L was resolved by SDS-PAGE and immunoblotted with phospho-Ser^{52}-hnRNP L or hnRNP L antibodies. (**C**) Exogenous hnRNP L phosphorylated by AKT competes with endogenous hnRNP U for binding to E3/C9. Recombinant hnRNP L was incubated with denatured or active AKT2 in the *in vitro* kinase assay and then utilized in the SBAP-based competitive binding assay using HBEpC cell lysates and E3/C9 ROs. (**D**) Model for controlling hnRNPU-hnRNP L-E3/C9 interaction by AKT pathway. In the non-transformed cells, the recruitment of hnRNP L to E3/C9 is interfered by hnRNP U binding to the same position. Through activation of AKT pathway in transformed cells, hnRNP L is phosphorylated, which results in the enhanced binding of this splicing repressor to E3/C9. Consequently, the elevated levels of hnRNP L associated with E3/C9 prevent the access of hnRNP U to E3/C9 for splice-enhancing function. The graphs shown in (A), (B) and (C) are representative of n=4 from two independent experiments.

CHAPTER 4 – DISCUSSION:
REGULATION OF CASPASE-9 SPLICING BY HNRNP U

In this study, two additional C9/E3-associated proteins were identified by LC-MS/MS, hnRNP R and hnRNP U. Whereas hnRNP R had no effect on caspase-9 splicing, hnRNP U was revealed as a splicing enhancer and validated for interaction with C9/E3. To date, little is known about the regulatory function of hnRNP U in RNA splicing although it is regarded as an RNA-binding protein. A recent study suggested that hnRNP U might be a global regulator of alternative splicing; however, >90% of reported cases about an RNA splicing change induced by hnRNP U down-regulation did not accompany binding to respective mRNA (69). Our findings expand the situations where hnRNP U-regulated splicing events are associated with target mRNA interactions.

The precise site for hnRNP U binding on C9/E3 was also examined. Previously, hnRNP U has been reported to preferentially bind G/U-rich motifs in RNA (19, 34). In line with these reports, hnRNP U was demonstrated to specifically interact with the G-rich sequence, GAGGG in C9/E3. Furthermore, mutation of the upstream U-motif (UUUGAGGG) also significantly reduced the association of hnRNP U with the C9/E3. Importantly, this sequence has been reported as a binding site for hnRNP L. The opposing function of hnRNP U versus hnRNP L and the same binding site on C9/E3 suggest regulatory competition between hnRNP U and hnRNP L

and our data further suggest that the presence of hnRNP U likely restricts the exon-exclusion effect of non-phosphorylated hnRNP L. Furthermore, the dramatic loss of protein:RNA complex by mutation of this RNA *cis*-element suggests that hnRNP L and U may target additional RNA trans-factors to exon 3. Current experimental directions are focused on determining whether the phosphorylation of hnRNP L leads to loss or gain of binding partners, which aid in regulating the inclusion/exclusion of the exon 3,4,5,6 cassette.

The nature of the regulation of the hnRNP U and L competition was also elucidated in this study. For example, simple changes in expression of the RNA *trans*-factors did not account for the observed loss of hnRNP U binding in transformed cells. Specifically, the expression of hnRNP U and L were not significantly different between non-transformed and transformed cells. Previous studies in our laboratory have pointed to the importance of phosphorylation in regulating hnRNP L-C9/E3 interaction (21), and hnRNP U has been reported to be selectively phosphorylated in response to DNA double-strand breaks (3, 6). Therefore, we hypothesized that phosphorylation events might impact the association between hnRNP U and C9/E3. Nevertheless, our findings in this study demonstrate that phosphorylation of hnRNP U is unlikely to play a role, and the regulatory mechanism is mainly via phosphorylation of hnRNP L. Together with the findings that caspase-9a/9b ratio is higher in non-transformed than in transformed cells (21, 57) and the enhanced association of hnRNP U in non-transformed cells, these data extend the mechanistic insights into the dysregulation of caspase-9 splicing in transformed cells. In this paradigm, certain survival/oncogenic kinases are activated and phosphorylate hnRNP L in transformed cells. As a result, the hnRNP L-C9/E3 interaction and subsequent splice-repressing function is promoted while hnRNP U is prevented from binding and competing with hnRNP L (Fig. 1.9D). Therefore, the exclusion of four-exon cassette is favored

shifting the alternative splicing of caspase-9 to the lower caspase-9a/9b ratio observed in NSCLC cells.

Since the enhanced exclusion of exon 3,4,5,6 cassette has been linked to phosphorylation events modulated by phosphoinositide 3-kinase/AKT pathway (Shultz 2010), this cell-survival regulatory pathway likely mediates the phosphorylation of hnRNP L and subsequently the competitive interaction between hnRNP L and hnRNP U to C9/E3. Indeed, inhibition of AKT signaling in transformed cells augmented hnRNP U-C9/E3 binding, and the enhanced binding to the C9/E3 were correlated perfectly with alteration in caspase-9 splice variant ratio. Hence, the AKT pathway regulates the alternative splicing of caspase-9 via hindering the interaction between hnRNP U and C9/E3 and subsequently suppressing its splice-enhancing function. Our study also demonstrates that hnRNP L is a direct substrate for AKT, and thus, AKT may be directly influencing the alternative splicing of caspase-9 via hnRNP L. Direct phosphorylation of hnRNP L by AKT is not heretical as AKT has been shown to directly phosphorylate SRSF1 (SRp30a or ASF/SF2), another RNA *trans*-factor known to regulate the alternative splicing of caspase-9 (57).

In regards to SRSF1 and caspase-9 RNA splicing, the presented study fills a missing "gap" in our knowledge of how the exon 3,4,5,6 cassette is regulated. Previously, we reported that the phosphorylation of SRSF1 on novel phosphorylation sites flanking the RS domain were partially required for AKT activation to exclude the exon 3,4,5,6 cassette (57). Specifically, we showed that a phospho-mimic of SRSF1 could only partially block the exclusion of the exonic cassette of caspase-9 pre-mRNA induced by an AKT inhibitor. This study now places hnRNP L phosphorylation and subsequent hnRNP U displacement from exon 3 as the plausible missing

mechanism by which AKT activation maximally induces the exclusion of the exon 3,4,5,6 cassette.

One of the more intriguing findings is the observation that phosphorylation of hnRNP L induces the association of the RNA *trans*-factor with a non-standard binding site. Numerous reports in the literature have demonstrated that hnRNP L prefers CA-repeats. Indeed, we initially found that recombinant hnRNP L did not bind the purine-sequence in-line with previous reports; however, hnRNP L can be modulated to associate with different sequence specificity by phosphorylation. Our data, therefore, suggest that hnRNP L may have both constitutive roles in RNA splicing as well as activated roles in modulating a subset of splicing events. How phosphorylation would change the sequence specificity of an RNA *trans*-factor has not been described, but possibly one or more qRRM motifs could be "unmasked" by an intra-molecular change in the structure of the RNA *trans*-factor stimulated by phosphorylation. This mechanism is plausible as hnRNP K, a related RNA *trans*-factor, has been reported to have a qRRM that does not recognize the standard GC-rich RNA sequence (46). Overall, phosphorylation may be a key regulatory step in activating RNA splicing factors to induce specific RNA splicing events (e.g. caspase-9 RNA splicing) in response to external stimuli outside of their roles in constitutive RNA splicing.

In conclusion, our presented work implicates hnRNP U as a limiting factor for caspase-9b formation, which has been previously demonstrated to enhance the anchorage-dependent growth and tumorigenic capacity of non-small cell lung cancer (NSCLC) cells (21). Moreover, cascape-9b is not significantly expressed in non-transformed cells (21), and the induction of caspase-9b expression is due to activation of hnRNP L via phosphorylation to compete/inhibit hnRNP U association with C9/E3. Therefore, targeting the phosphorylation of hnRNP L by specific kinase

inhibitors to further augment the formation of apoptotic caspase-9a over anti-apoptotic caspase-9b would be an attractive cancer-specific approach for treatment of NSCLC (50).

CHAPTER 5 – INTRODUCTION:
MECHANISTIC FUNCTIONS OF CASPASE-9B IN THE NF-KB PATHWAY

5.1 Caspase-9b

As presented in 1.3, the alternative splicing of caspase-9 leads to the formation of two splice variants and two corresponding isoforms, caspase-9a and caspase-9b. Lacking the catalytic site but still containing the CARD domain in the structure confers caspase-9b the anti-apoptotic capability (55, 59). Specifically, caspase-9b can bind to Apaf-1 via the CARD domain and competes with caspase-9a for Apaf-1 association. Protection against apoptosis is also the only-known function of caspase-9b. Recently, caspase-9b has been reported to enhance the anchorage-independent growth and tumorigenic capacity of NSCLC cells (21), which indicates that besides inhibiting apoptosis, caspase-9b may have activating roles in certain survival/oncogenic pathway(s). Understanding the mechanisms of how caspase-9b augments the anchorage-independent growth and tumorigenic capacity of NSCLC cells would have significant contribution to therapeutic development against lung cancer based on targeting caspase-9b.

5.2 NF-κB signaling: the canonical and non-canonical pathway

NF-κB refers to a family of transcription factors, Rel family, which plays important roles in various biological processes including inflammation, immune response, cell growth control, apoptosis and development (24, 64). In mammalian cells, five NF-κB

proteins have been identified: RelA (p65), RelB, c-Rel, NF-κB1 (p105/p50) and NF-κB2 (p100/p50). These NF-κB proteins form different homodimeric or heterodimeric complexes that can enter the nucleus, bind to the κB-enhancer sites and *trans*-activate numerous responsive genes. For structural comparison, all five NF-κB proteins share a unique N-terminal Rel homology domain (RHD) required for the formation of hetero- or homo-dimers and DNA binding. However, only RelA, RelB and c-Rel has C-teminal transactivation domain (TAD), which can activate the dimeric transcription factor complexes formed with p52 or p50. Since p52 and p50 both lacks TAD, their homo-dimers act as transcription repressors.

NF-κB dimers are normally sequestered in the cytoplasm by a family of inhibitors, comprising IκB-α, IκB-β, IκB-γ, IκB-ε, NF-κB1 p105 (precursor) and NF-κB2 p100 (precursor). The NF-κB inhibitors mask the nuclear localization signals (NLS) within NF-κB proteins and capture them in the cytoplasm. The precursor NF-κB1and NF-κB2, p105 and p100, have the IκB-like ankyrin-repeat domain, which thereby functions as NF-κB inhibitors. Proteosomal processing of p105 and p100 not only generates the active NF-κB1 p50 and NF-κB2 p52 but also abolishes the IκB-like action of the

precursor proteins.

There are two main arms of the NF-κB signaling, the canonical and noncanonical NF-κB pathway (Fig. 2.1). The canonical NF-κB pathway is activated by a broad range of stimuli such as inflammatory cytokines, lipopolysaccharides (LPS), growth factors or antigen receptors. The limiting step in the canonical NF-κB pathway is the inducible degradation of IκB proteins, particularly IκBα, which leads to nuclear transport of various NF-κB complexes, predominantly the RelA-containing dimer. Upon canonical NF-κB activation, IκB-α is phosphorylated by the IκB kinase (IKK), which is a trimeric complex

composed of two catalytic subunits, IKK-α and IKK-β, and a regulatory subunit, IKK-γ (or NF-κB essential modulator, NEMO). Phosphorylation of IκB-α results in its poly-ubiquitination and proteasome-mediated degradation. The non-canonical NF-κB pathway is signaled through particular TNF receptor family members that bind to the TNF receptor associated factors TRAF2 and/or TRAF3, such as LTβR, CD40, CD27, CD30, BAFF-R and RANK. Activation of the non-canonical pathway relies on NIK and IKKα-mediated phosphorylation and processing of NF-κB2 p100 precursor to p52, which then undergoes nuclear translocation of p52-containing dimers.

5.3 The roles of NF-κB activation in lung tumorigenesis and tumor progression

NF-κB is an inducible member of Rel family of transcription factors that regulate the expression of more than 200 genes, many of which encode for anti-apoptotic proteins such as Bcl-xL, cIAP1/2, A20, TRAF-2 and c-FLIP (32), regulatory factors in cell cycle control such as cyclin D (26) and GADD45 (10), angiogenesis factors such as VEGF (vascular endothelial growth factor), TNFα and MMPs (matrix metalloproteinases) (22, 42) and regulatory factors involved in cell migration and adhesion such as VCAM-1 (vascular cell adhesion molecule-1), ICAM-1 (intercellular adhesion molecule-1), CXCR4 (chemokine receptor) and uPA (serine protease urokinase-type plasminogen activator) (22, 42). Therefore, NF-κB signaling may be utilized by cancer cells to survive, proliferate, invade and metastasize. In fact, NF-κB pathway is constitutively activated in a variety of cancers, including prostate, breast, cervical, pancreatic and lung cancer (31, 40). Tumor samples from lung cancer patients present high levels of NF-κB activation in both small cell lung cancer (SCLC) and non-small cell lung cancer (NSCLC) (29, 31). Furthermore, it has been reported that NF-κB activation contributes to lung tumor formation and progression in mouse models (2, 14, 47) and also plays important roles in the invasion of

lung cancer cells (11, 27). In sum, the correlation between lung cancer development and NF-κB activation has been well-established.

5.4 Targeting NF-κB signaling for NSCLC treatment

Anti-cancer drugs have been showed to induce NF-κB activation in cancer cells, which contributes to chemoresistance in these cells (30, 52, 66). Hence, NF-κB pathway is now an attractive target for therapeutic design to sensitize cancer cells to apoptosis induced by chemical therapy or to limit cancer invasion and metastasis. Current NF-κB inhibitors include natural or synthesized compounds that target NF-κB signaling directly by targeting various components/steps in the NF-κB pathway (e.s., activation of IKK, degradation of IκBα, nuclear translocation and DNA binding of NF-κB complexes) or indirectly by targeting factors that suppress/activate the NF-κB pathway (e.s., tumor suppressor p53, aurora kinases, heat shock protein 90) (12). Several NF-κB inhibitors that sensitize lung cancer cells to chemical therapy and radiation treatment are listed in **Table 2.1.** Interestingly, RNA aptamer targeting NF-κB1 p50 has been shown to inhibit NF-κB activation in NSCLC cells A549 and sensitize the cells to apoptosis (48, 49). Nevertheless, there are concerns about using NF-κB inhibitors in cancer therapy: 1) suppression of NF-κB signaling may impair immunity since NF-κB pathway plays crucial roles in both innate and adaptive immunity; 2) the efficacy of NF-κB inhibitors varies in different cells and tissues; and 3) NF-κB inhibitors may have off-target effects (e.s., inhibition of NF-κB by proteasome inhibitors may affect the turnover of other proteins outside of NF-κB pathway). Tremendous efforts have been made to develop an effective and selective NF-κB inhibitor that can be used as a single or adjuvant agent to treat NSCLC.

5.5 Specific aims of the study

The previously observed promoting effect of caspase-9b on the anchorage-independent growth and tumorigenicity of NSCLC cells (21) leads to our hypothesis that caspase-9b activates certain survival/oncogenic pathway(s) besides inhibitory roles on caspase-9a activation. In this study, we found the survival/oncogenic NF-κB pathway as the potential target of caspase-9b. We also determined the mechanistic roles of caspase-9b on each arm of the NF-κB pathways, the canonical and non-canonical arm. We further examined the biological relevance of the functions of caspase-9b in the NF-κB pathway, particularly the effects on cell survival, anchorage-independent growth and tumorigenicity of NSCLC cells.

Table 2.1 NF-κB inhibitors sensitizing lung cancer cells to chemotherapeutics or ionizing radiation (12) μ

NF-κB inhibitors	**Correlative chemotherapeutics or ionizing radiation**
Genistein	Cisplatin, docetaxel
Embelin	Paclitaxel
Curcumin	Vinorelbine
Knockdown of p65	Adriamycin
Expression of IκBα	Paclitaxel
Expression of mutant IκBα (super repressor)	Cisplatin, gemcitabline, adriamycin, etoposide
β-lapachone, nimesulide and MG132, resveratrol, knockdown of TRAF2	Ionizing radiation

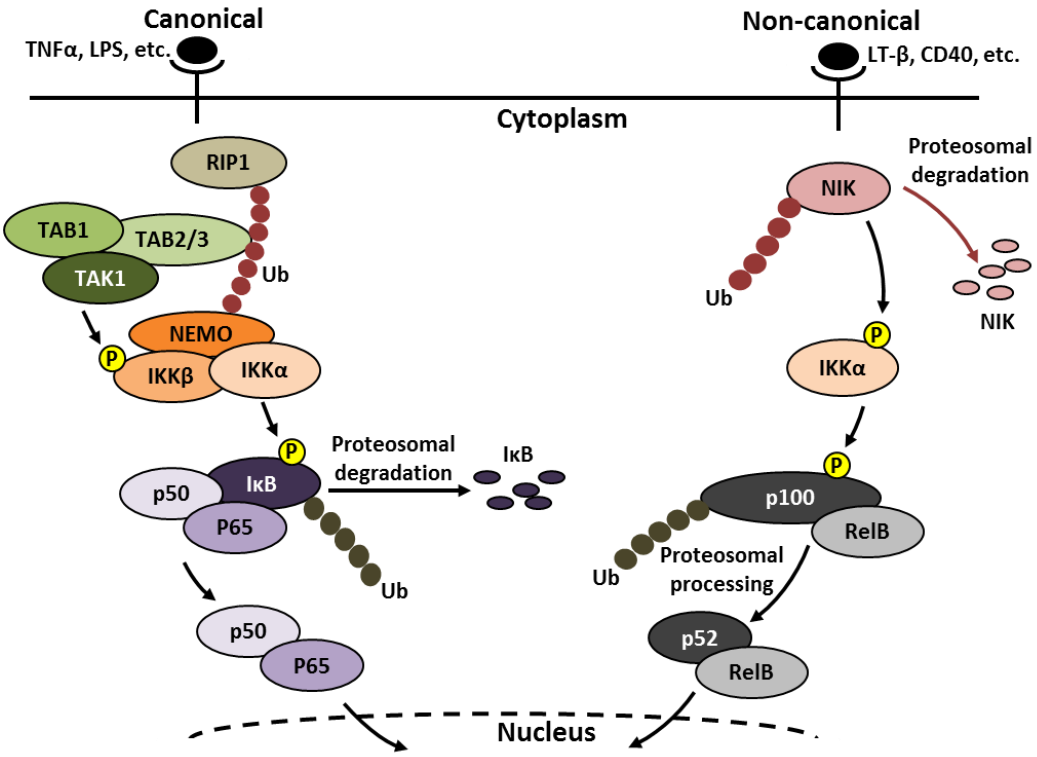

Figure 2.1 The canonical and non-canonical pathway in the NF-κB signaling. The limiting step in the canonical pathway is the proteosome-mediated degradation of IκB proteins, which allows the nuclear translocation of p65-containing complexes. In the non-canonical pathway, NF-κB activation is normally controlled by ubiquitination-mediated destabilization of NIK protein, which prevents the proteosomal processing of the NF-κB2 p100 to p52 and further inhibits the nuclear transport of p52-containing complexes.

CHAPTER 6 – MATERIALS AND METHODS: MECHANISTIC FUNCTIONS OF CASPASE-9B IN THE NF-KB PATHWAY

6.1 Cell culture

A549 and H838 lung adenocarcinoma cells were cultured in 50% DMEM and 50% RPMI medium with 10% (v/v) FBS (Sigma-Aldrich), 100 U/ml penicillin and 100 µg/ml streptomycin sulfate (Invitrogen). HEK 293 cells were cultured in DMEM medium with 10% (v/v) FBS (Sigma-Aldrich), 100 U/ml penicillin and 100 µg/ml streptomycin sulfate (Invitrogen). Human bronchial epithelial primary cells (HBEpC) were cultured in Bronchial/Tracheal Epithelial Cell Growth medium (Cell Applications). All cells were maintained at less than 80% confluency under standard incubator conditions.

6.2 siRNA transfection

A549, H838 or HBEpC cells were transfected with control siRNA or target siRNA for caspase-9a, caspase-9b or c-IAP1 (Dharmacon) using Dharmafect 1 transfection reagent (Dharmacon). Sequences of control or target si-RNA for caspase-9a or caspase-9b were listed in Table 2.2. Cells (3-4 x 10^5) were plated in each well of 6-well tissue culture dishes in regular growth medium. In the following day, cells were plated in Opti-MEM I medium without antibiotics/FBS and transfected with 50 nM (for c-IAP1) or 100 nM (for caspase-9a or caspase-9b) of siRNA (diluted in 1X siRNA buffer). In the next day, medium was changed to normal growth medium. After 24 hours, cells were collected for further analysis or transfected with adenovirus for additional 24 hours.

6.3 Next-Generation RNA Sequencing and Expression Analysis

RNAs extracted from the cells using the RNeasy Mini Kit (Invitrogen) were sent to Nucleic Acids Research Facilities, Virginia Commonwealth University, for Next-Generation Sequencing (deep RNA sequencing). FASTQ files were analyzed using the Galaxy software and Tuxedo protocol (62). Quality control of fragments was carried out using the FASTQC tool. Fragments were mapped to a reference genome using Tophat, and merged using Cuffmerge. BAM files were generated using Cufflinks and statistically significant transcripts were identified using Cuffdiff. Resulting files were analyzed using Ingenuity Pathway Analysis in order to identify differentially regulated pathways.

6.4 Plasmid transfection and selection of stable cell lines

Cell lines were transfected with plasmid vectors using Effectene Transfection Reagent (Qiagen Inc.) following the manufacturer's protocol. Briefly, cells were plated at approximately 40-60% confluency in 6-well plates or 100 mmm tissue culture dishes. The following day, cells were transfected with plasmid constructs. After 24 hours of standard incubation, cells were used in preparation of the protein extracts for Western immunoblotting or cell lysates for immunoprecipitation (IP)/co-immunoprecipitation (coIP).

For stable cell selection, cells were plated at $1.5x10^4$ cells in each well of 6-well plates. The following day, cells were transfected with 1ug of plasmid using Effectene Transfection Reagent (Qiagen Inc.). Cells were passaged into zeocin selection medium 24 hours after transfection and consistently treated with zeocin for 2 weeks.

6.5 Nuclear and cytoplasmic extraction

Cytoplasmic and nuclear extracts were separated and prepared from cells using NE-PER Reagents (Thermo scientific) following manufacture's protocol. For preparation of nuclear extract further used in DNA binding enzyme-linked immunosorbent assay (ELISA), the nuclear

pellet was resuspended in complete lysis buffer provided by the TransAM® NFκB p52/p65 ELISA Kits (Active Motif) instead of the NE buffer in the NE-PER Reagents (Thermo scientific).

6.6 Quantitative RT-PCR

Total RNA was extracted from the cells using the RNeasy Mini Kit (Invitrogen) and then reverse transcribed to cDNA using SuperScript III Reverse Transcriptase Kit (Invitrogen). The reverse transcription reaction products were utilized for real-time PCR for BIRC5, CXCR4, IRF3 and 18s using TaqMan PCR master mix and the Applied Biosystems 7500 Real-Time PCR System. ID numbers for BIRC5, CXCR4, IRF3 and 18s q-PCR primers (Applied Biosystems) were listed in Table 2.3. The relative amounts of BIRC5, CXCR4 and IRF3 were normalized to 18s.

6.7 DNA binding enzyme-linked immunosorbent assay (ELISA) for activated NFkB transcription factors

DNA-binding capacity of NF-κB p52- or p65-containing complexes were evaluated by using TransAM® NFκB p52/p65 ELISA Kits (Active Motif) and following the manufacturer's protocol. 5 μg of nuclear extract (in complete lysate buffer) was used for each well of the 96-well plate in which oligonucleotides containing NF-κB consensus binding site had been immobilized. The specific competitors (SC), which are the wild-type consensus oligonucleotides, and the non-specific competitors (NSC), which are the mutated consensus oligonucleotides, were utilized as the control for the specificity of the binding to the NF-κB consensus binding sequence. The Jurkat or Raji nuclear extract was used also as the positive control for p65 or p52 activation, respectively.

6.8 Immunoprecipitation (IP) and coimmunoprecipitation (coIP)

Cells were lysed in 1X coIP buffer containing 20 mM Tris-HCl pH 7.4, 150 mM NaCl, 1mM EDTA pH 8.0, 0.5% NP-40 and 1X phosphatase/protease inhibitor cocktail. Cells used for further immunoprecipitation of NIK were treated with 10 μM of proteasome inhibitor MG-132 for 1 hour before being lysed. For RIP, NIK or c-IAP1 immunoprecipitation/co-immunoprecipitation, 2 μl of RIP1, NIK or c-IAP1 monoclonal antibody was placed in each sample (0.5-1 mg of total proteins) for 4-5 hours at 4^{o}C with gentle agitation before 15 μl of pre-washed protein A/G magnetic beads (Thermo scientific) were added and incubated at room temperature for 10 minutes with gentle agitation. The bead complexes were washed 3 times with 1X coIP buffer, pelleted, resuspended in Laemmli buffer, incubated at room temperature for 10 minutes and the resulting supernatant were subjected to SDS-PAGE/immunoblotting. For myc or FLAG co-immunoprecipitation, 15ul of pre-washed anti-FLAG M2 magnetic beads (Sigma) or anti-Myc tag magnetic beads (Origene) were placed in each cell lysate sample for 3-4 hours at 4^{o}C with gentle agitation. The bead complexes were washed 3 times with 1X coIP buffer, pelleted and incubated with 60-80 μl of myc or 3X FLAG peptide (Sigma) solution for 45 minutes at 4^{o}C to elute the myc/FLAG fusion proteins. Final concentration of peptides in elution solution was 0.5 μg/ul in PBS with 1X phosphatase/protease inhibitor cocktail. The eluates were directly used in the *in vitro* ubiquitination assay or subjected to SDS-PAGE/immunoblotting.

6.9 Cell survival assay (colony formation assay)

Cells were trypsinized and 150 cells were plated in each well of the 6-well plates in normal growth medium (cells were plated on 3 wells for each occasion). Cells were incubated under standard incubator conditions for 10-14 days before the colonies were fixed with methanol and

stained with 0.05% crystal violet solution for 10 minutes. Then visually stained colonies were counted.

6.10 Colony formation assay in soft-agar

Cells were trypsinized and a total of 2,000 cells in 1ml top agar (normal growth media containing 0.35% agarose) were plated over 1.5 ml base agar layer (normal growth media containing 0.6% agarose) in each well of 6-well plates (cells were plated on 3 wells for each occasion). Cells were incubated under standard incubator conditions for 4 weeks before the colonies were stained with 0.005% crystal violet for 1 hour. Stained colonies with diameters larger than 100 μm were counted under a dissecting microscope. For colony size distribution, images from each well of the soft-agar plates were taken and image J program was used to calculate the average size of colonies.

6.11 *In vitro* ubiquitination assay

FLAG tagged cIAP1 or myc tagged wild-type/mutant caspase-9b was purified by immunoprecipitation of FLAG or myc fusion proteins from HEK 293 cells transfected with FLAG tagged cIAP1 plasmids or myc tagged wild-type/mutant caspase-9b plasmids for 24 hours in normal growth medium and placed in serum-free medium for additional 6 hours. Purified products of FLAG or myc immunoprecipitation from HEK 293 cells transfected with parental empty plasmids were utilized also as the negative control. *In vitro* ubiquitination reactions were performed at 37^{o}C for 1 hour. The reaction mixtures (20 μl) included 50 nM E1 (Boston Biochem E-305), 0.5 μM Ubc H5a E2 (E2-616), 1 μl FLAG tagged cIAP1 as E3 ligase or FLAG negative control, 8 μl myc-tagged wild-type/mutant caspase-9b or myc negative control, 100 ng recombinant tagged RIP1 (Abcam), 10 μM ubiquitin (Boston Biochem), 5 mM ATP, 50 mM

Tris 7.5, 5 mM $MgCl_2$ and 2 mM DTT. After incubation time, the product mixtures were analyzed by Western immunoblotting.

6.12 Animals and tumor models

Six-week-old male C.B-17 SCID (IcrHsd-*Prkdc*^{scid}) mice were purchased from Harland. Animal experiments were conducted at Virginia Commonwealth University. The research protocol (protocol number AD10000534) was approved by the VCU IACUC involving animal care in accordance with the US Department of Agriculture (USDA) Animal Welfare Regulations, the Public Health Service Policy on the Humane Care and Use of Laboratory Animals, and the US Government Principles for the Utilization and Care of Vertebrate Animals Used in Testing, Research, and Training. VCU is in compliance with all provisions of the Animal Welfare Act and other federal statues and regulations relating to animals. VCU is registered under the Animal Welfare Act as a class R research facility with the USDA Animal and Plant Health Inspection Service (APHIS) Animal Welfare (registration number 52-R-0007). The Office of Laboratory Animal Welfare (OLAW) approved the VCU Animal Welfare Assurance in compliance with the Public Health Service Policy (assurance number A3281-01). The SCID mice were acclimatized to the VCU Medical School Animal Facility for a week before they received injections of cancer cells: $1.1x10^6$ A549 human NSCLC cells were resuspended in 100 μl DMEM and injected subcutaneously into the right hind flank. Tumors were allowed to develop for up to 4 weeks and tumor size was measured every week by using a caliper. After 4 weeks, mice were sacrificed and tumors were extracted and weighed.

6.13 Statistical analysis

Statistical differences between 2 objects were determined by a 2-tailed, unpaired Student's *t* test. Statistical differences among more than 3 objects were evaluated by one-way ANOVA

followed by a Tukey's HSD test. *p* values of less than or equal to 0.05 were considered significant.

6.14 Adenovirus information

Adenovirus control (Vector Biolabs, catalog number 1300), adenovirus expressing IκB-α (Vector Biolabs, catalog number 1504) or dominant negative IκB-αS (Vector Biolabs, catalog number 1028) were used at 20-50 MOI. Adenovirus control or expressing caspase-9b were used at 5 MOI for HBEpC cells, at 10 MOI for H838 cells and at 20-50 MOI for A549 cells. Higher virus titer was used in A549 cells to obtain relatively the same level of protein expression.

6.15 Antibody information

The following antibodies were used in western immunoblotting, immunoprecipitation (IP) or co-immunoprecipitation (co-IP): anti-caspase-9 (Assay Designs), anti-p65 (Cell Signaling Technology), anti-NF-κB2 (Cell Signaling Technology), anti-IκB-α (Cell Signaling Technology), phospho-IκB-α (Cell Signaling Technology), anti-β-actin (Sigma), anti-laminA/C (Cell Signaling Technology), anti-α-tubulin(Cell Signaling Technology), anti-NIK (Cell Signaling Technology), anti-RIP1 (Cell Signaling Technology), anti-ubiquitin (Cell Signaling Technology), anti-cIAP1 (Cell Signaling Technology), anti-Apaf1 (Cell Signaling Technology), anti-FLAG (Sigma), anti-myc (Cell Signaling Technology), horseradish peroxidase-conjugated anti-rabbit IgG antibody (Cell Signaling Technology) and horseradish peroxidase-conjugated anti-mouse IgG antibody (Cell Signaling Technology)

Table 2.2 Control si-RNA for caspase-9a or caspase-9b, caspase-9a si-RNA and caspase-9b si-RNA utilized in the study.

si-RNA name	**Sequence**
• Random control	GGAAUUCCAUCUAGCUCAAACUU
• Mutant caspase-9a control, a mixture of 3 siRNA:	
○ Mutant caspase-9a 1	ACCAGUGGCACUACUGCGGUUUU
○ Mutant caspase-9a 2	CAUCAGAAGAACUGCGGUGAGUU
○ Mutant caspase-9a 3	CACUAGACGCGUGAGGCCAGGUU
• Mutant caspase-9b control	GUAUAGGACAUCACGACGAUAUU
• Caspase-9a, a mixture of 3 siRNA:	
○ Caspase-9a 1	AACAAUGUGAACUUCUGCCGUUU
○ Caspase-9a 2	AAUGUGAACUUCUGCCGUGAGUU
○ Caspase-9a 3	AACUUCUGCCGUGAGUCCGGGUU
• Caspase-9b	GAUUUGGUGAUGUCGAGCAUUUU

Table 2.3 qPCR primers specific for NF-κB target genes.

Gene	**ID number**
BIRC5	*Hs04194392_s1*
CXCR4	*Hs00607978_s1*
IFR3	*Hs01547283_m1*
18S	*Hs99999901_s1*

CHAPTER 7 – RESULTS:
MECHANISTIC FUNCTIONS OF CASPASE-9B IN THE NF-KB PATHWAY

7.1 Identification of NF-κB as the signaling pathway of caspase-9b target

Until now, the only-known function of caspase-9b is protection against apoptosis by inhibition of caspase-9a processing (44, 48). Since expression of caspase-9b has previously demonstrated to augment tumorigenicity of NSCLC cells, caspase-9b expression might have a "gain of function" phenotype or in other words, activate survival/oncogenic pathways outside of its inhibitory effect on caspase-9a function. Therefore, high throughput next-generation sequencing (deep RNA sequencing) has been performed to identify cell signaling pathways as plausible targets of caspase-9b and deep RNA sequencing analysis has revealed a potential link between caspase-9b and the NF-κB pathway. Specifically, down-regulation of caspase-9b affects expression of various genes, which have been shown in literature to be related to the up-stream or down-stream of the NF-κB pathway (figure 2.2 and table 2.4). Furthermore, nearly 40% of these genes are NF-κB responsive genes (table 2.5). The finding of NF-κB as a potential pathway of caspase-9b target suggests that caspase-9b might regulate the survival/oncogenic NF-κB pathway and affecting the NF-κB pathway might contribute to caspase-9b-mediated enhancement of tumorigenic capacity of NSCLC cells.

7.2 Caspase-9b activates the canonical and inhibits the noncanonical NF-κB pathway

The roles of caspase-9b in the NF-κB signaling were further validated. In the NF-κB pathway, p65- or p52-containing complexes are the dominant complexes in the canonical or noncanonical arm and activation of the canonical or noncanonical arm leads to the nuclear transport of p65 or p52 complexes, respectively. As shown in figure 2.3A and B, knocking down of caspase-9b resulted in less p65 but more p52 translocated into the nucleus and expressing caspase-9b increased the nuclear p65 level but decreased the level of nuclear p52. In correlated with the nuclear translocation, caspase-9b impacts, in a contrasting manner, the expression of the canonical versus non-canonical NF-κB target genes (figure 2.3C and D). More p65 or less p52 in the nucleus of the caspase-9b-reduced cells also leads to more p65 or less p52 binding to DNAs containing NF-κB responsive sites (figure 2.3E and F). Together, these findings indicate the opposite roles of caspase-9b in two arms of the NF-κB pathway, activating the canonical and inhibiting the noncanonical arm.

The limiting step in the canonical NF-κB pathway is the phosphorylation-mediated turn-over of IκB proteins, particularly IκB-α, whereas activation of the noncanonical pathway relies on stabilization of NIK and processing of NF-κB2 p100 precursor to p52. Hence, NF-κB2 p100 processing and the level of IκB-α and NIK were evaluated when caspase-9b is up- or down-regulated. As a result, caspase-9b was shown to dramatically promote the the processing of NF-κB2 p100, phosphorylation and degradation of IκB-α (figure 2.4A and B). Caspase-9b was also shown to impact the ubiquitination and turn-over of NIK (figure 2.4C, D and E). Since it has been reported that NIK is tightly controlled by ubiquitination- and proteasome-mediated degradation (41), the observed increase in NIK level (figure 2.4C and D) and decrease in NIK ubiquitination (figure 2.4E) as caspase-9b is down-regulated supports our model where caspase-

9b prevents the noncanonical NF-κB activation by elevating the ubiquitination and degradation of NIK. Caspase-9b down-regulation not only affected NIK ubiquitination, it also decreased RIP1 ubiquitination (figure 2.4E). RIP1 is a crucial factor in the NF-κB signaling, of which ubiquitination has been known to positively regulate the canonical NF-κB pathway (15, 33, 67), contrary to ubiquitination of NIK and consequent non-canonical NF-κB repression (41). Therefore, these findings further solidify the dual actions of caspase-9b in the NF-κB signaling: on one hand, caspase-9b stimulates RIP1 ubiqutination and enhances phosphorylation-mediated degradation of the IκB-α, freeing p65-containing complexes to translocate into the nucleus for gene transcription; on the other hand, caspse-9b facilitates ubiquitination-mediated degradation of NIK and thereby prevents the processing and nuclear transport of the NF-κB2, which then keeps the non-canonical NF-KB in an off-state.

7.3 Caspase-9b enhances the survival and anchorage-independent growth (AIG) capability of NSCLC cells by activation of the canonical NF-κB pathway

Caspase-9b expression has been demonstrated to promote the anchorage-independent growth (AIG) and tumorigenic capacity in NSCLC cells (21). In accordance with the literature, down-regulation of caspase-9b resulted in a decrease of cell survival and stable expression of caspase-9b increased the survival of NSCLC cells (figure 2.5A and B). Due to the activating roles of caspase-9b in the oncogenic/survival NF-κB pathway, i.e. the canonical pathway, it is likely that activation of the canonical NF-κB contributes to the enhancement of cell survival by caspase-9b. In order to address that hypothesis, the NF-κB suppressor IκB-α or the dominant-negative suppressor (or super repressor), IκB-αS, was expressed in the NSCLC cells followed by expression of caspase-9b. Repression of the canonical NF-κB by expression of the suppressor or super suppressor both led to a significant decrease in cell survival and only the suppressing effect

of the IκB-α on the survival was rescued by caspase-9b expression (figure 2.5C). Additionally, caspase-9b expression enhanced the degradation of IκB-α but had no effect on IκB-αS level (figure 2.5C), which might explain the rescue of cell survival by caspase-9b expression only toward IκB-α expression. Another approach was utilized to determine the biological relevance of the NF-KB activating roles of caspase-9b, particularly focusing on the cell survival and AIG: the suppressor or super suppressor was expressed in the control cells or cells stably expressing caspase-9b. For the control cells, expression of either suppressor IκB-α or super suppressor IκB-αS resulted in a decrease of colony formation in both conditions, with or without soft-gar but for the cells stably expressing caspase-9b, only expression of the non-degradable IκB-αS reduced the number of colonies formed (figure 2.5D). Importantly, cells stably expressing caspase-9b had lower level of IκB-α but the same level of IκB-αS compared to control cells (figure 2.5D), which is in agreement with all findings above and the hypothesis that caspase-9b augments the cell survival and AIG by facilitating degradation of IκB-α and consequent canonical NF-κB activation.

7.4 cIAP1 plays critical roles in caspase-9b-mediated NF-κB activation/inhibition

The roles of caspase-9b in both canonical and non-canonical NF-κB pathway give rise to a possibility that caspase-9b might interact with certain regulatory factors that mediate the cross-talk between two arms of the signaling pathway. In this regard, cellular inhibitors of apoptosis (cIAPs) are of interest since c-IAP proteins have been known to have functions in both canonical and non-canonical pathway (5, 28, 44, 64, 65, 71). Validated by our study, down-regulation of c-IAP1 had similar effects as caspase-9b on the NF-κB signaling. c-IAP1 down-regulation increased the processing of the NF-κB2 p100 to p52 and the level of both NIK and IκB-α (figure 2.6A). Furthermore, c-IAP1 depletion altered the level of nuclear p65 and p52, specifically

decreased p65 and increased p52 level (figure 2.6B). Down-regulation of c-IAP1 also reduced the ubiquitintation of RIP1 and NIK (figure 2.6C). All of these findings indicate that c-IAP1 might mediate the effects of caspse-9b on NF-KB signaling and the lung cancer cell survival.

The above hypothesis was supported by results showing that down-regulation of c-IAP1 abolished the activating/inhibitory effects of caspase-9b on the NF-KB pathway, particularly the level of NIK and IκB-α (figure 2.7A and B) and the ubiquitination of RIP1 and NIK (figure 2.7C). Importantly, c-IAP1 depletion also abrogated the enhanced cell survival conferred by caspase-9b expression (figure 2.7D). Taken together, it is likely that c-IAP1 mediates the action of caspase-9b on the NF-κB signaling to enhance the survival of NSCLC cells.

7.5 Caspase-9b directly binds to c-IAP1

Several proteins of the inhibitor of apoptosis protein (IAP) family members, particularly XIAP and c-IAP1/2, have been known to associate with the processed caspase-9 via the IAP-binding motif (IBM) motif on caspase-9 (16, 59). This four-residue motif has been conserved during evolution and it is also present in the IAP-interacting protein Smac/DIABLO of human/mice and in a group of pro-apoptotic factors, Reaper, head-involution defective (Hid), Grim and sickle (Skl), of Drosophila (hence, also known as Reaper–Hid–Grim, RHG, motif) (59). The truncated caspase-9b still retains the IBM and thereby possibly binds to c-IAP1 to modulate the NF-κB signaling. This possible direct interaction was validated by coimmunoprecipitation of the endogenous c-IAP1 and ectopically expressed caspase-9b (figure 2.8A). Furthermore, mutation on caspase-9b at IBM (sequence shown in figure 2.8B) reduced the association between c-IAP1 and caspase-9b (figure 2.8C) but did not interfere with the interaction between caspase-9b and Apaf-1 (figure 2.8D), which suggests that mutant caspase-9b is structurally intact and IBM on caspase-9b is crucial for c-IAP1 binding. Interestingly, although

caspase-9 has been reported to bind to XIAP or c-IAP1/2 only if being processed (16, 59), our results indicate that full-length caspase-9b (37 KDa) still binds to c-IAP1. Additionally, mutations of caspase-9b at the cleavage sites had no effects on its interaction with c-IAP1 (figure 2.9A). It is plausible that whereas caspase-9 needs to be cleaved to expose the IBM for c-IAP1/2 binding, the truncated caspase-9b has already had the IBM exposed; thus, no more processing is necessary.

The residue(s) on c-IAP1 required for caspse-9b binding has also been revealed. It has been reported that residues in BIR2 and BIR3 domain of c-IAP1 are critical for caspase-9 interaction (16). Therefore, these residues were mutated to examine if they are also required for caspase-9b binding (sequences indicated in figure 2.10A). Interestingly, only one out of four mutations, mutation at D320 on BIR3 of c-IAP1, was shown to abolish caspase-9 binding. Importantly, D320A mutation did not affect c-IAP1 interaction with RIP1 (figure 2.10B), which ruled out the possibility that D320A mutation impaired the whole c-IAP1 structure. These findings point to the importance of residue(s) on BIR3 domain of c-IAP1 for interaction with caspase-9b.

7.6 Caspase-9b regulates the NF-κB pathways and promotes the survival and tumorigenicity of NSCLC cells via direct interaction with c-IAP1

To examine whether the association of caspase-9b to c-IAP1 is essential for caspase-9b-mediated NF-κB activation/inhibition, mutated caspase-9b at IBM, which was showed to have remarkably reduced binding to c-IAP1 (figure 2.8C), was expressed and NIK/IκB-α level was evaluated. As shown in figure 2.11A, expression of IBM-mutated caspase-9b did not significantly affect NIK and IκB-α level as expression of wild-type caspase-9b. This finding was congruent with the observation that mutation of caspase-9b at cleavage site(s), which was not shown to affect caspase-9b binding to c-IAP1, was also not shown to affect the capability of

caspase-9b to regulate NIK and IκB-α level (figure 2.9B). Mutation of caspase-9b at IBM also resulted in loss of enhancing effect of caspase-9b on the survival (figure 2.11B) and AIG of NSCLC cells (figure 2.11C). At tumor formation level, NSCLC cells expressing wild-type caspase-9b formed tumors in mice with dramatically higher volume and weight compared to control cells or cells expressing mutated caspase-9b (figure 2.11D). Most important, only expression of wild-type caspase-9b but not of mutated caspase-9b rescued the reduced survival and AIG of NSCLC cells as a result of caspase-9b depletion (figure 2.11E, F and G). Overall, via binding to c-IAP1, caspase-9b affects both arms of the NF-κB signaling and enhances the survival and tumorigenicity of the NSCLC cells.

7.7 Caspase-9b augments the E3 ligase activity of c-IAP1

Given that the E3 ligase activity of c-IAP1 impacts ubiquitination of RIP1 and ubiquitination-mediated degradation of NIK (4, 5, 64, 71), caspase-9b likely binds to c-IAP1 and promotes its E3 ligase activity. Supporting to this plausible mechanism, co-expression of wild-type caspase-9b and c-IAP1 was showed to induce the ubiquitination of RIP1 and NIK in a significantly higher magnitude than expression of either wild-type caspase-9b or c-IAP1 alone (figure 2.12A and B). Addition of caspase-9b into the *in vitro* ubiquitination assay dramatically increased the E3 ligase activity of c-IAP1 (figure 2.12C). Furthermore, the enhancing effect of caspase-9b on c-IAP1-mediated ubiquitination was diminished when caspase-9b/c-IAP1 binding was interfered by mutation of caspase-9b at IBM (figure 2.12A, B and C). These findings shed light on how interaction between c-IAP1 and caspase-9b facilitates the roles of caspase-9b in the NF-κB pathways: through binding to c-IAP1, caspase-9b enhances its E3 ligase activity to induce ubiquitination of RIP1 for the canonical NF-κB activation and ubiquitination of NIK for turning off the non-canonical pathway (figure 2.12D).

Table 2.4 List of NF-κB-related genes that expression is affected by down-regulation of caspase-9b (identified by deep RNA sequencing analysis)

Gene name	Gene ID
BAD	572
BAX	581
BCL2A1	597
BCL2L1	598
BCL2L2	599
BIRC2	329
BIRC3	330
BMI1	648
C3	718
CASP8	841
CCL2	6347
CCL3	6348
CCL5	6352
CCNB2	9133
CCND1	595
CD44	960
CDC25B	994
CDKN1A	1026
CFLAR	8837
CLU	1191
CREB3	10488
CSNK2A1	1457
CXCL1	2919
CXCL2	2920
CXCL3	2921
CXCL8	3576
CXCL10	3627
ELF3	1999
EMR1	2015
ERAP1	51752
ERBB2	2064
FAS	355
FTH1	2495
FUCA1	2517
GDF15	9518
HMOX1	3162
ICAM1	3383
IER3	8870
IFNL1	282618
IL15RA	3601
IRF1	3659
IRF7	3665

JUNB	3726
LITAF	9516
MCL1	4170
MICA	100507436
MYC	4609
NAMPT	10135
NFKB2	4791
NFKBIA	4792
NFKBIZ	64332
NOP14	8602
PLAU	5328
PLK1	5347
PTGS2	5743
RRAS2	22800
SDC4	6385
SENP1	29843
SENP2	59343
SMAD3	4088
SOAT1	6646
SOCS1	8651
SOCS3	9021
SOD2	6648
TCF12	6938
TFPI2	7980
TGFB1	7040
TGM2	7052
TNFAIP8	25816
TNFRSF10B	8795
TNFRSF1A	7132
TNIP1	10318
TP53	7157
TRAF2	7186
TRIB3	57761
WTAP	9589
XIAP	331

Table 2.5 List of NF-κB target genes that expression is affected by down-regulation of caspase-9b (identified by deep RNA sequencing analysis)

Gene name	Gene ID
BAX	581
BCL2A1	597
BCL2L1	598
BMI1	648
C3	718
CCL2	6347
CCL3	6348
CCL5	6352
CCND1	595
CD44	960
CDKN1A	1026
CFLAR	8837
CREB3	10488
CXCL1	2919
CXCL3	921
CXCL10	3627
ELF3	1999
ERAP1	51752
ERBB2	2064
FAS	355
FTH1	2495
HMOX1	3162
ICAM1	3383
IER3	8870
IRF1	3659
IRF7	3665
JUNB	3726
MICA	100507436
MYC	4609
NAMPT	10135
NFKB2	4791
NFKBIA	4792
NFKBIZ	64332
NOP14	8602
PLAU	5328
PTGS2	5743
SDC4	6385
SENP2	59343
SOD2	6648
TFPI2	7980
TGM2	7052
TNFAIP8	25816

TNFRSF10B	8795
TNFRSF1A	7132
TNIP1	10318
TP53	7157
TRAF2	7186
XIAP	331

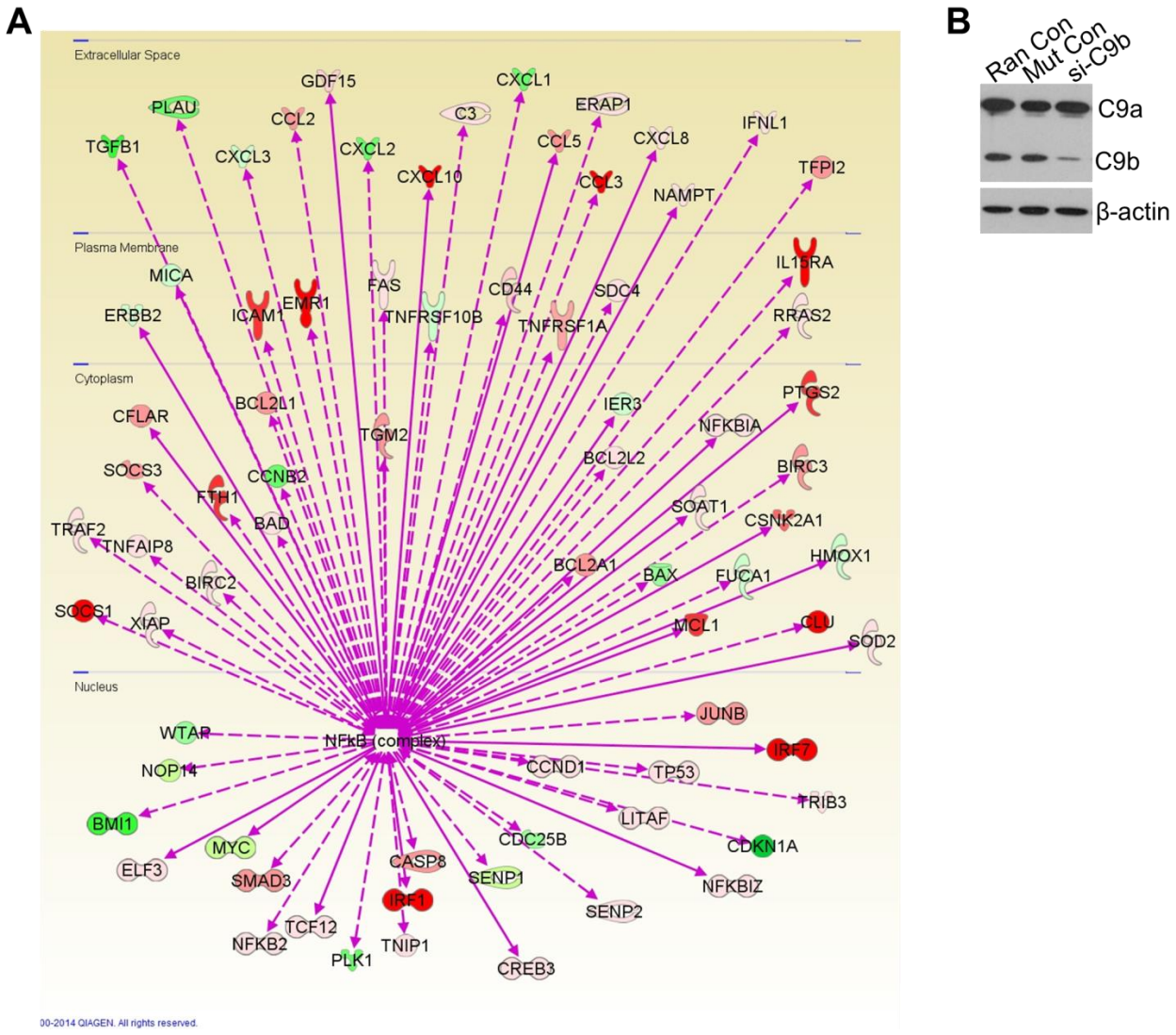

Figure 2.2 Deep sequencing reveals NF-κB as the signaling pathway affected by caspase-9b. A549 cells were transfected with random control, mutant caspase-9b control or caspase-9b siRNA for 48 hours. (**A**) Total RNA were isolated and analyzed by deep RNA sequencing. The graph represents all NF-κB-related genes, of which expression was significantly different between control samples (random or mutant caspase-9b) and caspase-9b-down-regulated samples. Red, up-regulated genes; green, down-regulated genes; higher color intensity indicates higher difference in expression level; solid line arrows, genes/factors directly affecting/affected by NF-κB transcription complexes; dashed line arrows, genes/factors indirectly affecting/affected by NF-κB transcription complexes. Cell localization of these NF-κB-related factors was also indicated. (**B**) Total proteins were prepared and subjected to SDS-PAGE/immunoblotting for caspase-9 or β-actin. The graphs shown in (A) and (B) are representative of n=4 from two independent experiments.

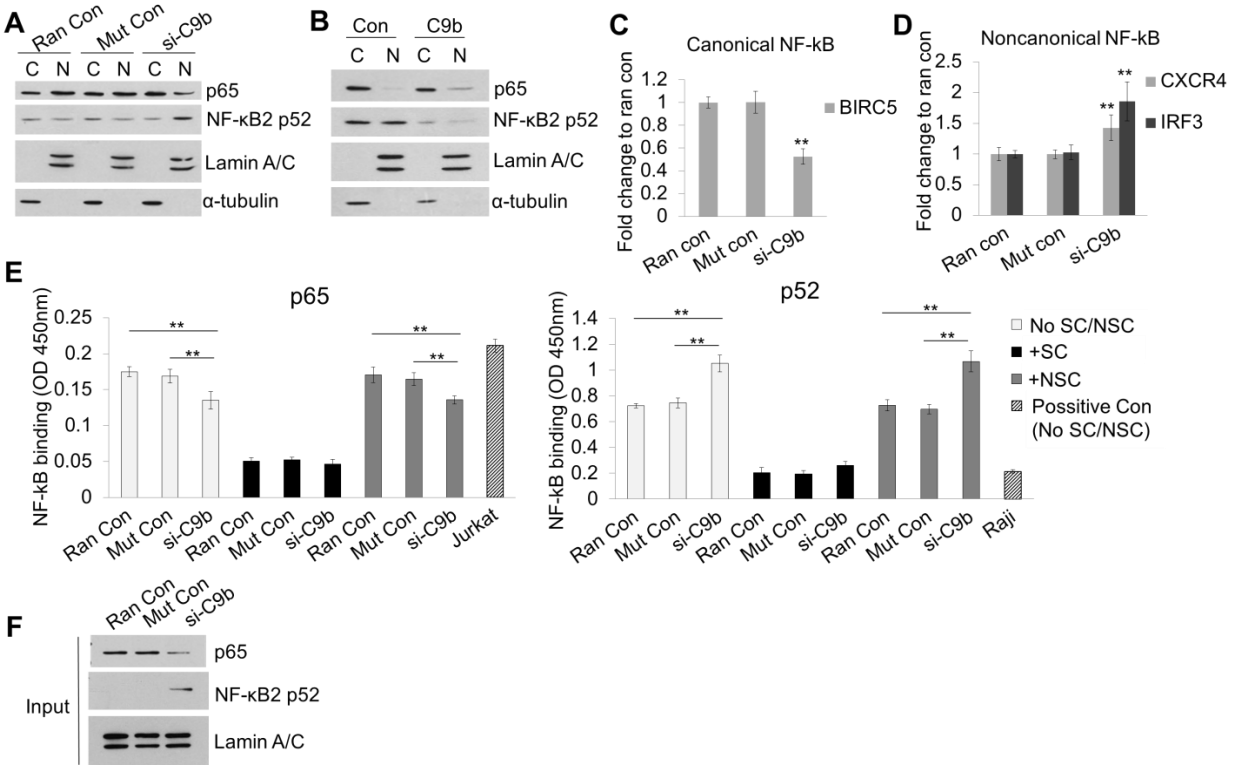

Figure 2.3 Caspase-9b affects expression of NF-κB target genes, nuclear translocation and DNA binding activity of NF-κB proteins. (**A and B**) Caspase-9b has effects on the nuclear transport of p65 and p52. (A) Cytosolic/ nuclear fractions were prepared from A549 cells transfected with random control, mutant caspase-9b control or caspase-9b siRNA for 48 hours (A) and from A549 control cells or cells stably expressing caspase-9b (B). Cytosolic/nuclear protein extracts were subjected to SDS-PAGE/immunoblotting for NF-κB p65, NF-κB2, lamin A/C or α-tubulin. (**C and D**) Caspse-9b affects the expression of NF-κB target genes. Total RNA was isolated from A549 cells transfected with random control, mutant caspase-9b control or caspase-9b siRNA and relative amount of the canonical (A) or noncanonical (B) NF-κB targets was determined by quantitative RT-PCR. (**E**) DNA binding ELISA for NF-κB p65 or p52 were performed using nuclear extracts from A549 cells transfected with random control, mutant caspase-9b control or caspase-9b siRNA for 48 hours. Specific or nonspecific competitors (SC or NSC) were also utilized. Nuclear extracts from Jurkat or Raji cells were used as positive control for p65 or p52 activation. (**F**) Nuclear extract input in (E) was subjected to SDS-PAGE/immunoblotting for NF-κB p65, NF-κB2 or lamin A/C. Data are shown as means ± SD (n=6 on 2 independent occasions). Statistical significance was evaluated by one-way ANOVA followed by a Tukey's HSD test (#p<0.05, ##p<0.01, *p<0.005, **p<0.001). Experiments in (A) and (B) were repeated at least twice.

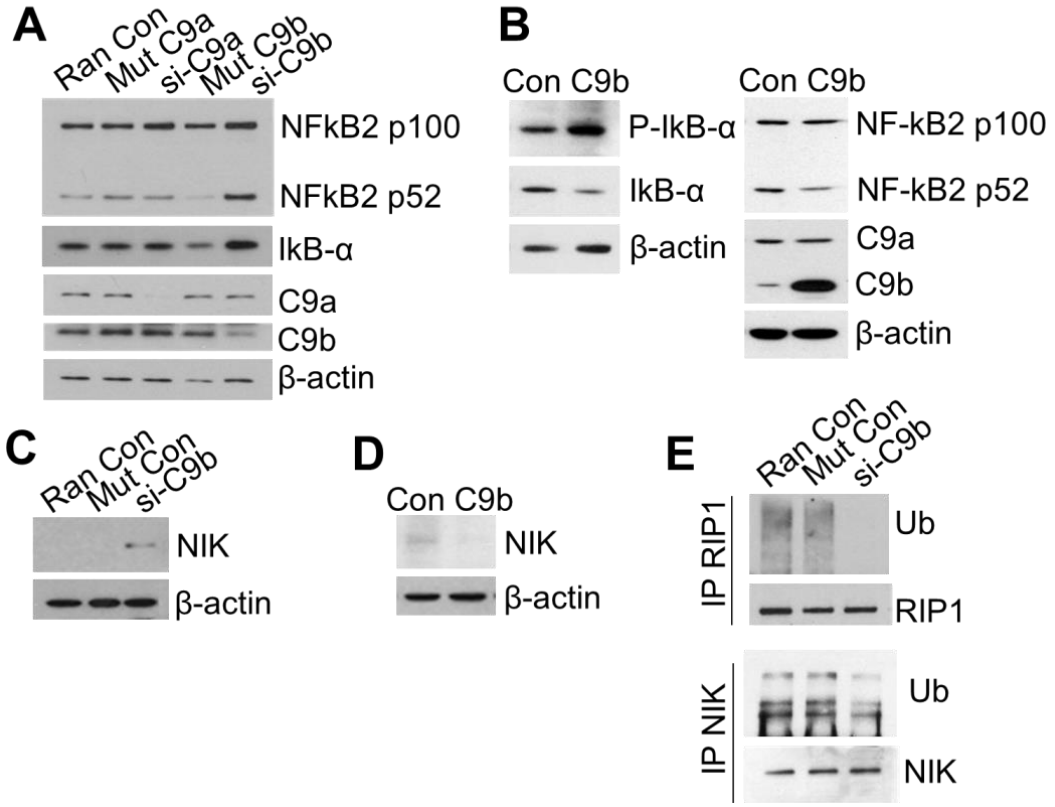

Figure 2.4 Caspase-9b promotes the processing, turn-over and ubiquitination of proteins in the NF-κB signaling. (**A and C**) Down-regulation of caspase-9b increases the processing of NF-κB2 p100 to p52 and the level of IκB-α (A) as well as NIK protein (C). A549 cells transfected with random control, mutant caspase-9a control, caspase-9a, mutant caspase-9b or caspase-9b siRNA for 48 hours. Total protein extracts were subjected to SDS/PAGE/immunoblotting for NF-κB2 p100/p52, IκB-α, caspase-9, NIK or β-actin. (**B and D**) Caspase-9b expression decreases the processing of NF-κB2 p100 to p52 and the level of IκB-α (B) as well as NIK protein (D). A549 cells were transfected with parental empty or C9b-expressing plasmids for 24 hours. Total protein extracts were subjected to SDS/PAGE/immunoblotting for NF-κB2 p100/p52, phospho-IκB-α, IκB-α, caspase-9, NIK or β-actin. (**E**) Down-regulation of caspase-9b decreases the unbiquitination of RIP1 and NIK proteins. A549 cells were transfected with random control, mutant caspase-9b control or caspase-9b siRNA for 48 hours. Endogenous RIP1or NIK was immunoprecipitated (IP) from cell lysates and resolved by SDS-PAGE/ immunoblotting for ubiquitin, RIP1 or NIK. All experiments were repeated at least twice.

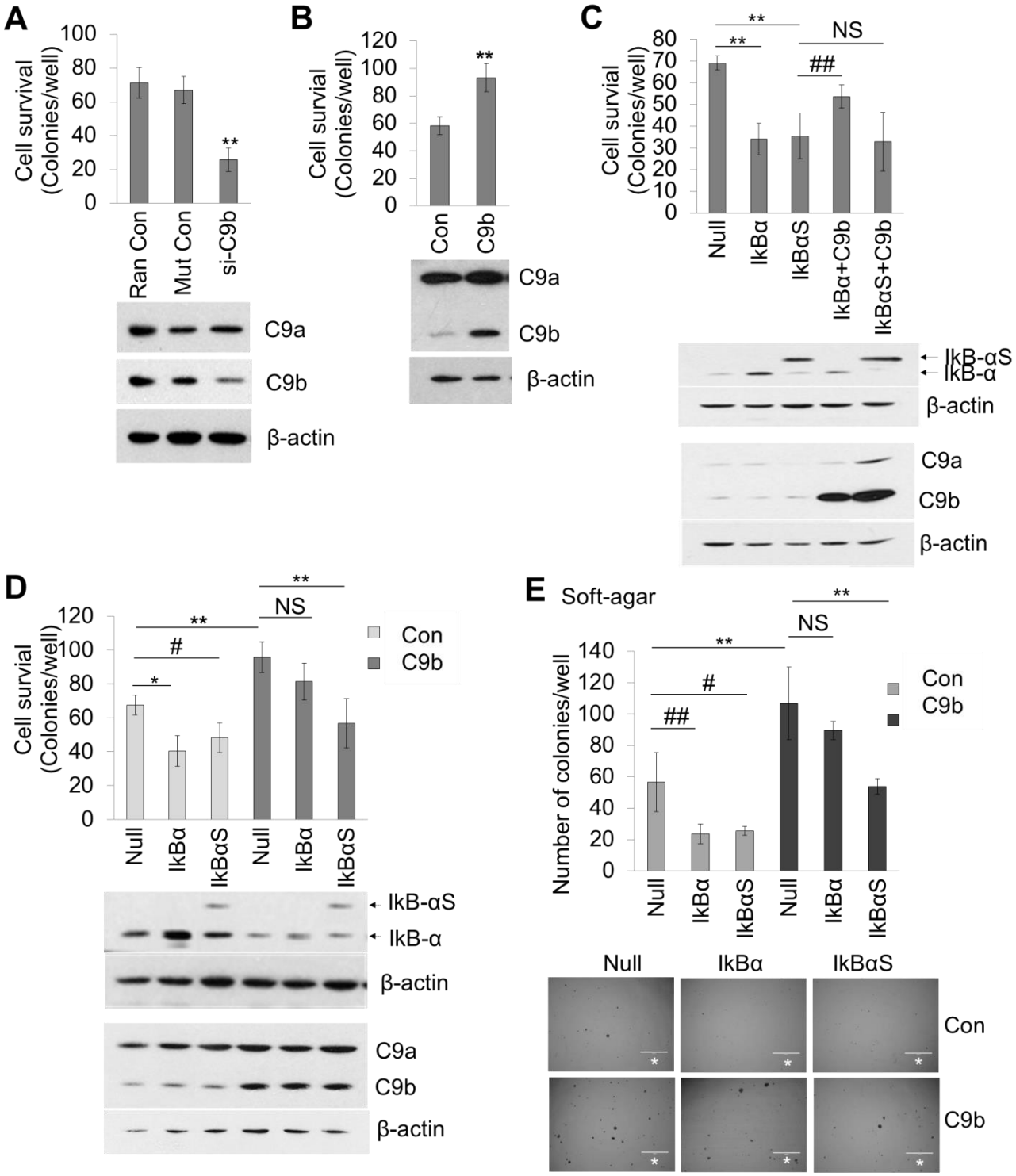

Figure 2.5 Activation of the canonical NF-κB pathway contributes to caspase-9b-mediated enhancement of the survival and anchorage-independent growth of NSCLC cells. (**A, B, C and D**) Colony formation assays were performed with A549 cells transfected with random control, mutant caspase-9b control or caspase-9b siRNA for 48 hours (A), with A549 control or

caspase-9b-stably-expressing cells (B), with A549 cells transfected with control adenovirus or adenovirus expressing IκB-α or super suppressor IκB-α (IκB-αS) for 24 hours followed by 24-hour transfection with control adenovirus or adenovirus expressing caspase-9b (C), with A549 control or caspase-9b-stably-expressing cells transfected with control adenovirus or adenovirus expressing IκB-α or super suppressor IκB-α (IκB-αS) for 24 hours (D). Western immunoblotting of total protein extracts from cells in each case were also performed for caspse-9, IκB-α, IκB-αS or β-actin. (E) Colony formation assays in soft-agar were carried out using A549 cells as in (D). The graph presents the average number of colonies on each well of the 6-well plates. Representative fields of the soft-agar plates were shown in the microscopic images below the graphs, (*) scale bar, 2 mm. Data are shown as means ± SD (n=6 on 2 independent occasions). Statistical significance was evaluated by one-way ANOVA followed by Tukey's HSD test (#p<0.05, ##p<0.01, *p<0.005, **p<0.001).

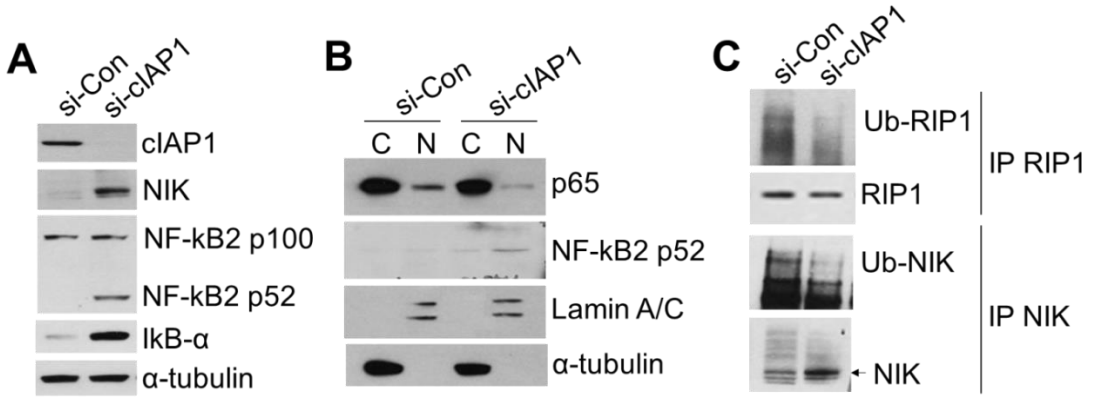

Figure 2.6 Down-regulation of cIAP1 has similar effects on the NF-κB pathway with down-regulation of caspase-9b. A549 cells were transfected with control or c-IAP1 siRNA for 48 hours. (**A**) Total protein extracts were prepared and subjected to SDS/PAGE/immunoblotting for cIAP1, NIK, NF-κB2 p100/p52, IκB-α or β-actin. (**B**). Cytosolic/nuclear protein extracts were prepared and subjected to SDS-PAGE/immunoblotting for NF-κB p65, NF-κB2, lamin A/C or α-tubulin. (**C**) Endogenous RIP1or NIK was immunoprecipitated (IP) from cell lysates and resolved by SDS-PAGE/ immunoblotting for ubiquitin, RIP1 or NIK. All experiments were repeated at least twice.

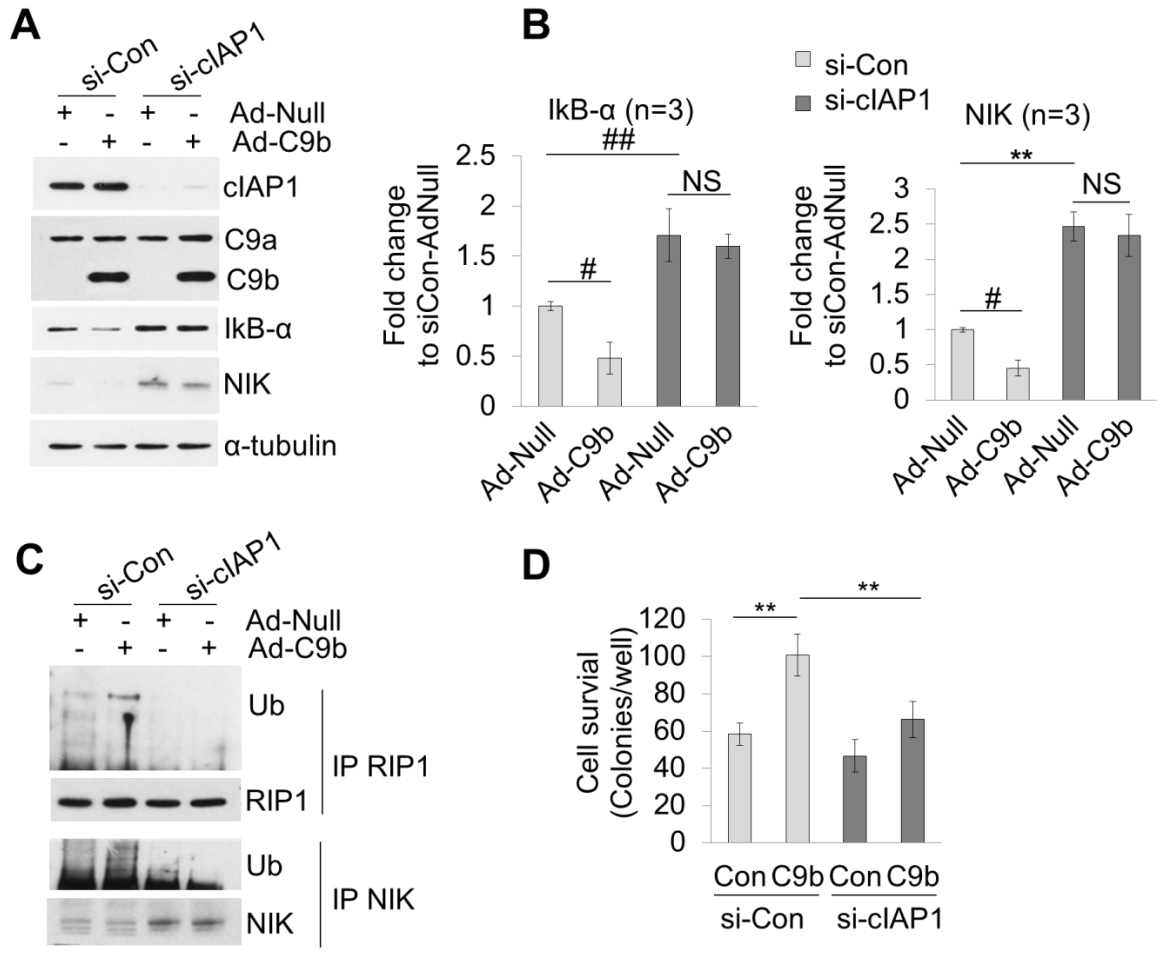

Figure 2.7 Down-regulation of cIAP1 abrogates the activating/inhibitory effect of caspase-9b on the NF-κB signaling. A549 cells were transfected with control or c-IAP1 siRNA for 48 hours followed by 24-hour transfection with control adenovirus or adenovirus expressing caspase-9b. (**A**) Total protein extracts were prepared and subjected to SDS/PAGE/immunoblotting for cIAP1, caspase-9, IκB-α, NIK or β-actin. (**B**) Graphs were created by densitometry calculation of the results in (A). Data in (B) are shown as means ± SD (n=3). Statistical significance was evaluated by one-way ANOVA followed by a Tukey's HSD test (#p<0.05, ##p<0.01, *p<0.005, **p<0.001). (**C**) Endogenous RIP1or NIK was immunoprecipitated (IP) from cell lysates and resolved by SDS-PAGE/ immunoblotting for ubiquitin, RIP1 or NIK. (**D**) Colony formation assays were carried out from the above cells. Data in (D) are shown as means ± SD (n=6 on 2 independent occasions). Statistical significance was evaluated by one-way ANOVA followed by Tukey's HSD test (#p<0.05, ##p<0.01, *p<0.005, **p<0.001). Experiments in (A), (B) and (C) were repeated at least twice.

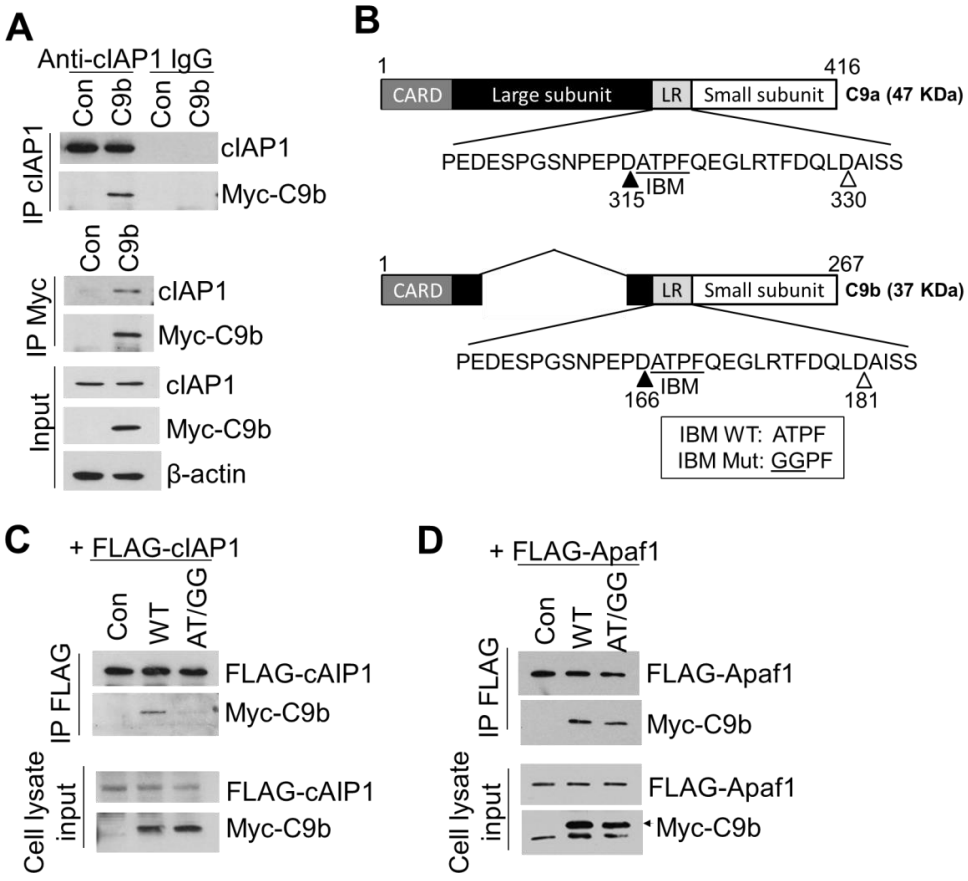

Figure 2.8 Caspase-9b directly binds to c-IAP1 via the IAP-binding motif. (**A**) Caspase-9b associates with cIAP1. A549 cells were transfected with parental empty plasmid or plasmid expressing myc-tagged caspase-9b. Endogenous cIAP1 or myc-tagged caspase-9b was coimmunoprecipitated (coIP) from cell lysates and resolved by SDS-PAGE/ immunoblotting for c-IAP1 or myc. Input was immunoblotted for c-IAP1, myc or β-actin. IgG was also used as the control. (**B**) Schematic representation of protein structure for caspase-9a and caspse-9b. Compared to caspase-9a, caspase-9b lacks most of the large subunit, including the catalytic site, but retains the caspase recruitment domain (CARD), linker region (LR) and small subunit. The LR contains the cleavage sites (closed triangle indicates the auto-cleavage site and opened triangle indicates the site for caspase-3-mediated cleavage) and a conserved IAP-binding motif (IBM). Sequences of the wild-type (WT) and mutated (Mut) IBM utilized the study were indicated in the text box. (C and D) Mutation at IBM disrupts caspase-9b binding to c-IAP1 but not to Apaf-1. (**C**) A549 cells were co-transfected with FLAG-tagged cIAP1 and parental empty plasmid or plasmid expressing myc-tagged wild-type (WT) or mutated caspase-9b at the IBM for 24 hours. FLAG-tagged cIAP1 was coimmunoprecipitated (coIP) from cell lysates and resolved by SDS-PAGE/ immunoblotting for FLAG or caspase-9. (**D**) A549 cells were co-transfected with FLAG-tagged Apaf-1 and parental empty plasmid or plasmid expressing myc-tagged wild-type (WT) or mutated caspase-9b at the IBM for 24 hours. FLAG-tagged Apaf-1 was coimmunoprecipitated (coIP) from cell lysates and resolved by SDS-PAGE/ immunoblotting for FLAG or caspase-9. All experiments were repeated at least twice.

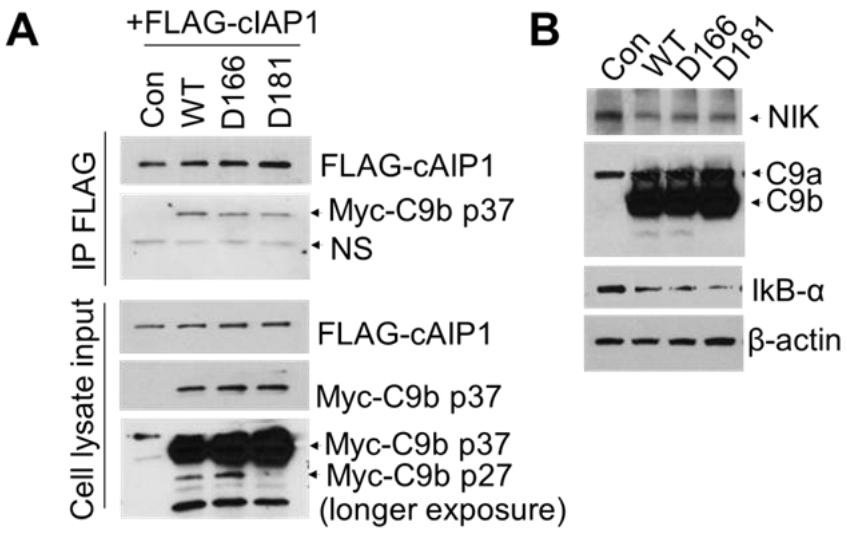

Figure 2.9 Cleavage of caspase-9b is unimportant for interaction with cIAP1. (A) A549 cells were co-transfected with FLAG-tagged cIAP1 and parental empty plasmid or plasmid expressing myc-tagged wild-type (WT) or mutated caspase-9b at the cleavage sites (D166A, D181A) for 24 hours. FLAG-tagged cIAP1 was coimmunoprecipitated (coIP) from cell lysates and resolved by SDS-PAGE/ immunoblotting for FLAG or caspase-9. Myc tagged full-length caspase-9b (37 KDa, p37) can be cleaved into p10 and myc tagged p27 subunit (if being cleaved at D166 site) or into p12 and myc tagged p25 subunit (if being cleaved at D181 site). NS, non-specific band. (**B**) A549 cells were transfected with parental empty plasmid or plasmid expressing myc-tagged wild-type (WT) or mutated caspase-9b at the cleavage sites for 24 hours and total protein extracts were prepared and subjected to SDS/PAGE/immunoblotting for NIK, caspase-9, IκB-α or β-actin. All experiments were repeated at least twice.

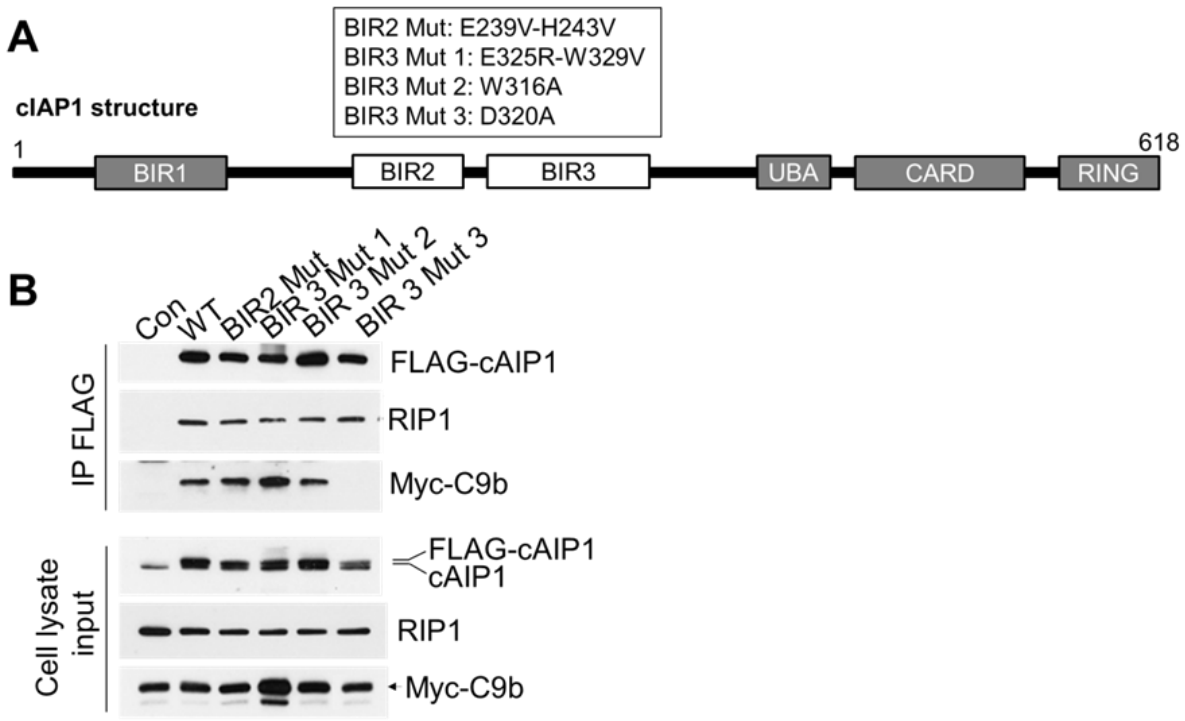

Figure 2.10 A residue in BIR3 domain of cIAP1 is critical for the association with caspase-9b. (A) Schematic of c-IAP1 structure. Critical residues for caspase-9 binding have been identified mostly in the BIR2 and BIR3 domain of c-IAP1 (white rectangles). c-IAP1 mutations utilized in the study were indicated in the text box. (B) A549 cells were co-transfected with myc-tagged caspase-9b and parental empty plasmid or plasmid expressing FLAG-tagged wild-type (WT) or mutated (Mut) cIAP1 in BIR2 domain or BIR3 domain for 24 hours. FLAG-tagged cIAP1 was coimmunoprecipitated (coIP) from cell lysates and resolved by SDS-PAGE/ immunoblotting for cIAP1, RIP1 or caspase-9. Experiments were repeated at least twice.

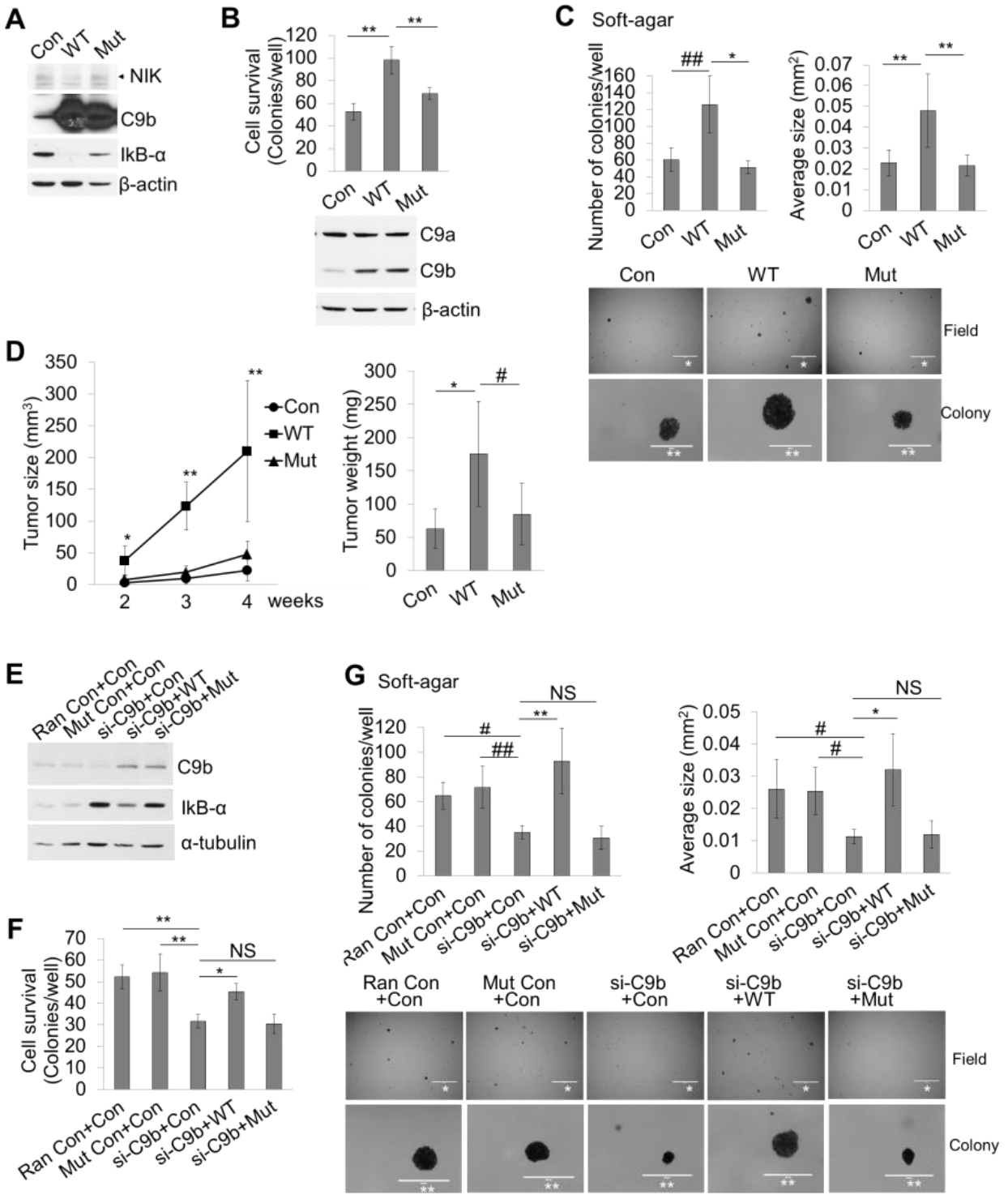

Figure 2.11 Direct binding to cIAP1 is essential for caspase-9b-mediated NF-κB activation/inhibition. (**A**) A549 cells were transfected with parental empty plasmid or plasmid expressing myc-tagged wild-type (WT) or mutated caspase-9b at IBM for 24 hours and total protein extracts were prepared and subjected to SDS/PAGE/immunoblotting for NIK, caspase-9, IκB-α or β-actin. (**B**) Colony formation assays were performed from stable control cells (A549)

or cells stably expressing myc-tagged wild-type (WT) or mutated caspase-9b at IBM. (**C**) Colony formation assays on soft agar were carried out using cells as in (B). The graphs present the colony size distribution and the average number of colonies on each well of the 6-well plate. Representative fields of the soft-agar plates and representative colonies were shown in the microscopic images below the graphs, (*) 2 mm scale bar, (**) 400 μm scale bar. (**D**) Cell lines in (B) or (C) were injected into right flanks of the SCID mice (1.1×10^6 cells/mice). Tumor size was measured every week. After 4 weeks, mice were sacrificed and tumor weight was evaluated. Data are shown as mean ± SD (n=8). Statistical significance was evaluated by one-way ANOVA followed by Tukey's HSD test (For the left graph, *p<0.005, **p<0.001, WT caspase-9b versus control or mutated caspase-9b; for the right graph, #p<0.05, *p<0.005). (E, F and G) A549 cells were transfected with random control, mutant caspase-9b control or caspase-9b siRNA for 48 hours followed by 24 hour transfection with parental empty plasmid or caspase-9b-siRNA-resistant plasmid expressing myc-tagged wild-type (WT) or mutated caspase-9b. (**E**) Total protein extracts were prepared and subjected to SDS/PAGE/immunoblotting for caspase-9, IκB-α or β-actin. (**F**) Colony formation assays were performed. (**G**) Colony formation assays on soft agar were carried out as in (C). Data are shown as means ± SD (n=5 for experiments in panel B and n=6 for experiments in panel C, F and G). Statistical significance was evaluated by one-way ANOVA followed by Tukey's HSD test (#p<0.05, ##p<0.01, *p<0.005, **p<0.001).

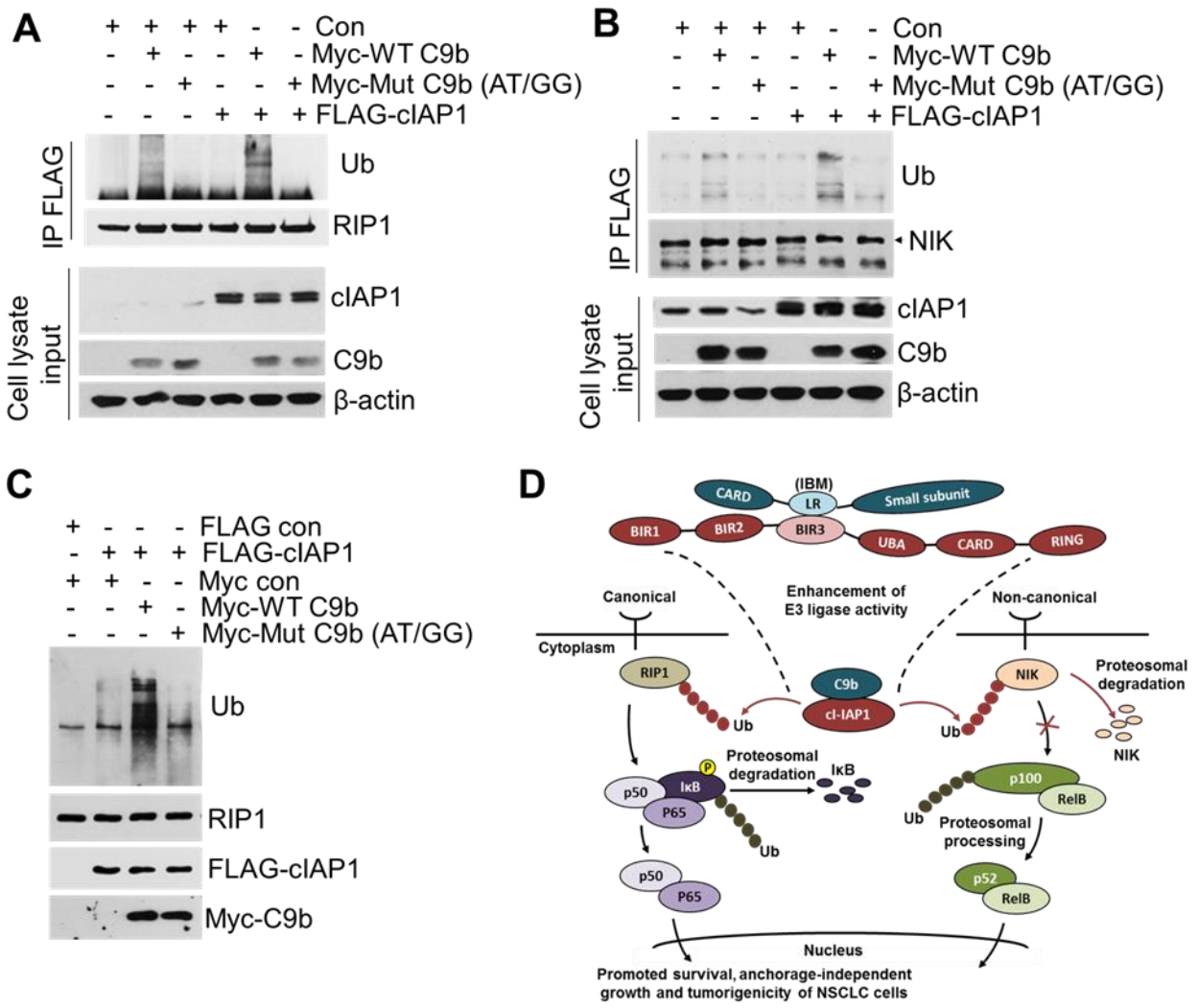

Figure 2.12 Caspase-9b enhances E3 ligase activity of c-IAP1 via direct interaction. (**A and B**) Caspase-9b/cIAP1 binding increases the ubiquitination of RIP1 (A) and NIK (B). A549 cells were transfected with a combination of parental control plasmid/ plasmid expressing FLAG-tagged cIAP1 and myc-tagged wild-type (WT)/mutated (Mut) caspase-9b at IBM for 24 hours. FLAG-tagged cIAP1 was coimmunoprecipitated (coIP) from cell lysates and resolved by SDS-PAGE/ immunoblotting for ubiquitin, RIP1 or NIK. Input was immunoblotted for c-IAP1, caspase-9 or β-actin. (**C**) Wild-type caspase-9b but not IBM-mutated caspase-9b increases E3 ligase activity of c-IAP1. *In vitro* ubiquitination assay was performed using E1 activating enzyme and E2 conjugating enzyme in the presence or absence of FLAG tagged cIAP1 (E3 ligase) and myc tagged wild-type (WT) or mutated (Mut) caspase-9b. FLAG tagged cIAP1, myc tagged WT or Mut caspase-9b was purified by immunoprecipitation (IP) of FLAG/myc fusion proteins from cells transfected with plasmid expressing FLAG-cIAP1 or myc-WT/Mut caspase-9b. In the absence of FLAG-cIAP1 or myc-WT/Mut caspase-9b, FLAG- or myc-immunoprecipitated products from cells expressing parental empty plasmid were used as controls. (**D**) Mechanistic model of how caspase-9b regulates the NF-κB signaling and promotes the survival and anchorage-independent growth capacity of NSCLC cells. In this model, caspase-9b directly binds to c-IAP1 via the IBM on caspase-9b and residue(s) on BIR3

domain of c-IAP1. Caspase-9b/c-IAP1 association enhances the E3 ligase activity of c-IAP1, which further elevates ubiquitination of RIP1 and NIK. Ubiquitination of RIP1 stimulates phosphorylation and ubiquitination-mediated degradation of IκB-α, allowing the p65-containing complexes to translocate into the nucleus and activation of the canonical NF-κB. Via canonical NF-κB activation, caspase-9b promotes the survival and anchorage-independent growth capacity of NSCLC cells. In contrast, ubiquitination destabilizes NIK, which prevents the processing of NF-κB2, nuclear transport of p52-containing complexes and the non-canonical NF-κB activation. All experiments were repeated at least twice.

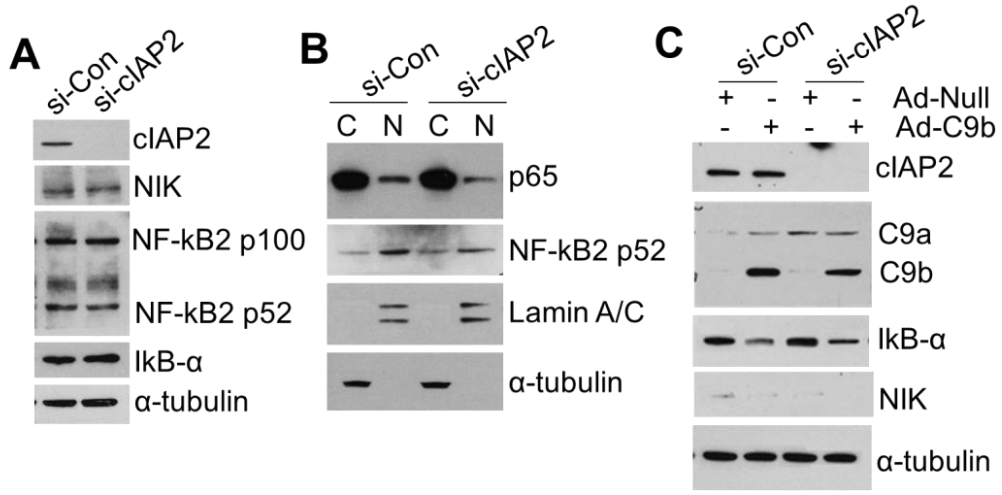

Figure 2.13 Down-regulation of cIAP2 has no effect on NF-κB activation and does not inhibit the effect of caspase-9b on NF-κB pathway. A549 cells were transfected with control or c-IAP2 siRNA for 48 hours. (**A**) Total protein extracts were prepared and subjected to SDS/PAGE/immunoblotting for cIAP2, NIK, NF-κB2 p100/p52, IκB-α or β-actin. (**B**) Cytosolic/nuclear protein extracts were prepared and subjected to SDS-PAGE/immunoblotting for NF-κB p65, NF-κB2, lamin A/C or α-tubulin. (**C**) Endogenous RIP1or NIK was immunoprecipitated (IP) from cell lysates and resolved by SDS-PAGE/ immunoblotting for ubiquitin, RIP1 or NIK.

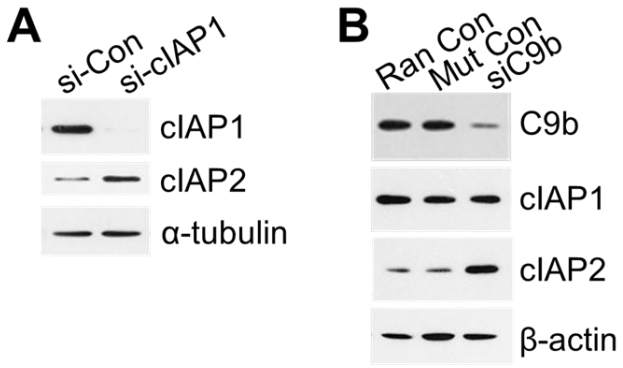

Figure 2.14 Down-regulation of c-IAP1 increases in c-IAP2 level. (**A**) A549 cells were transfected with control or c-IAP1 siRNA for 48 hours. Total protein extracts were prepared and subjected to SDS/PAGE/immunoblotting for cIAP1, c-IAP2 or β-actin. (**B**) A549 cells were transfected with random control, mutant caspase-9b control or caspase-9b siRNA for 48 hours. Total protein extracts were prepared and subjected to SDS/PAGE/immunoblotting for caspase-9, cIAP1, c-IAP2 or β-actin.

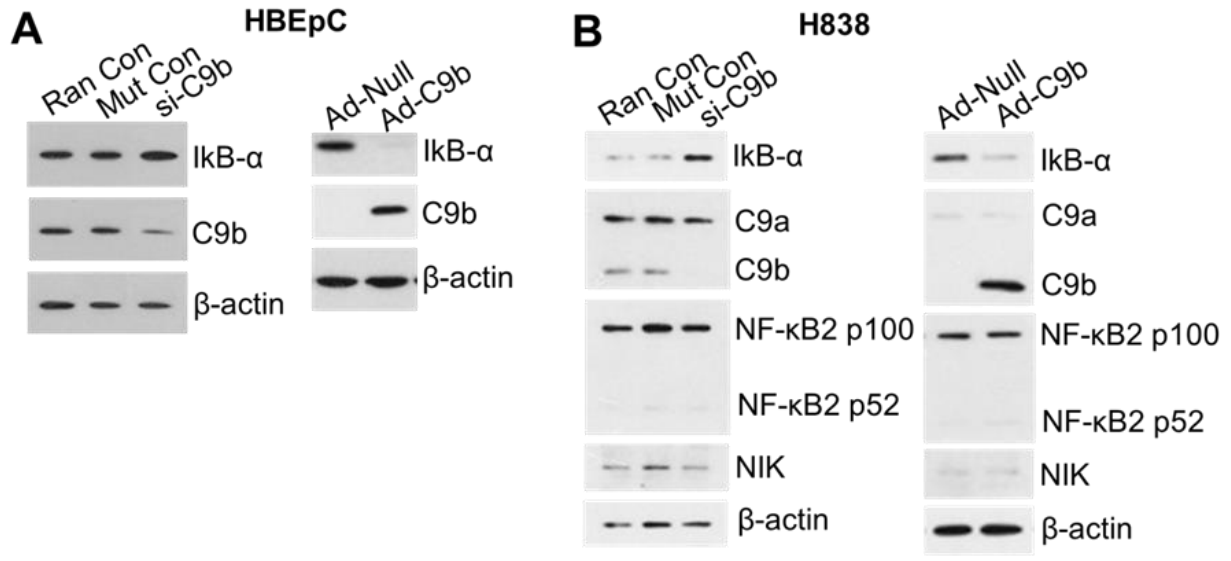

Figure 2.15 The role of caspase-9b in the NF-κB pathway examined in other cell lines. Human bronchial epithelial primary cells (HBEpC) (**A**) or lung cancer H838 cells (**B**) were transfected with random control, mutant caspase-9b control or caspase-9b siRNA for 48 hours. Total protein extracts were prepared and subjected to SDS/PAGE/immunoblotting for NF-κB2 p100/p52, IκB-α, caspase-9, NIK or β-actin. NF-κB2 p52 were undetectable in HBEpC.

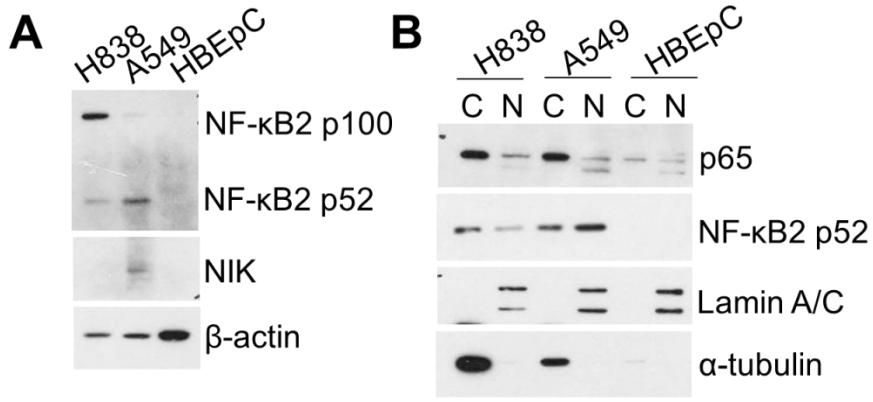

Figure 2.16 NF-κB activation in H838, A549 and HBEpC cells. A549 (mutant K-ras, wild-type p53), H838 (wild-type K-ras, wild-type p53) and HBEpC cells were cultured under the same and confluency. (**A**) Total protein extracts were subjected to SDS-PAGE/immunoblotting for NF-κB2, NIK or β-actin. **(B)** Cytosolic/ nuclear fractions were prepared and cytosolic/nuclear protein extracts were subjected to SDS-PAGE/immunoblotting for NF-κB p65, NF-κB2, lamin A/C or α-tubulin.

CHAPTER 8 – DISCUSSION:
MECHANISTIC FUNCTIONS OF CASPASE-9B IN THE NF-KB PATHWAY

Despite the well-documented function of caspase family in the initiation and execution of apoptosis, several studies have implicated caspases in the activation of anti-apoptotic NF-κB pathway. Caspases known to activate NF-κB signaling include caspase-1, -2, -8, -10 (9, 37, 38, 56). The role of caspase-9 in NF-κB activation remains controversial since the CARD domain of caspase-9 has been validated to enhance NF-κB activity (61) but in another report, caspase-9 has not been shown to activate NF-κB pathway (9). Particular to caspase-9b isoform, there is not convincing evidence for its correlation with NF-κB activation and generally, little is known about mechanistic roles of caspase-9b outside of its only-known function in inhibition of caspase-9a. Importantly, up-to-date studies regarding the mechanistic functions of caspases in NF-κB signaling focus mainly on the canonical pathway. Our study emphasized the roles of caspase-9b in both arms of the NF-κB signaling, the canonical and noncanonical pathway.

Caspase-9b was demonstrated to activate the canonical NF-κB pathway, the only arm of the NF-κB signaling reported to promote tumor development in NSCLC (2, 47). Consistent with the literature, activation of the canonical NF-κB was shown to mediate the enhancing effects of caspase-9b on the survival and anchorage-independent growths of NSCLC cells. To date, the majority of studies regarding the contribution of NF-κB signaling to tumorigenesis focus on canonical NF-κB pathway and the roles of non-canonical NF-κB pathway in lung cancer

development have not been specifically investigated. Caspase-9b regulates both arms of the NF-κB pathways in the opposite manner, giving rise to an idea that the non-canonical pathway might negatively affect tumor-promoting roles of the canonical pathway or activation of the canonical pathway. Supporting this hypothesis, non-canonical activation has been observed to prevent canonical activation in different ways (1, 39). There is likely a functional interplay between the two pathways to fine-tuning the gene transcription activity. Nevertheless, it is unlikely that the noncanonical pathway is a compensatory redundant mechanism for the canonical pathway due to the observation that when activation of the noncanonical pathway was favored as a result of caspase-9b downregulation, there was a significant decrease in the survival and anchorage-independent growth of NSCLC cells. It is plausible that under the suppressed condition of the canonical arm, the non-canonical arm is activated to maintain a basal level of NF-κB activity but it is for other biological functions rather than cell survival and growth in an anchorage-independent manner.

NF-κB activation has been implicated in cancer development and resistance to anti-cancer drugs (30, 52, 66). NF-κB pathway is thereby an attractive target for cancer therapeutic design. Caspase-9b was observed in this study to enhance the survival and anchorage-independent growth of NSCLC cells via direct association with c-IAP1 and activation of the canonical NF-κB pathway. Hence, targeting NF-κB signaling through interfering caspase-9b-c-IAP1 interaction would be a promising approach to inhibit the canonical NF-κB pathway and further compromise lung cancer development. An alternative approach to reduce canonical NF-κB activation is lowering caspase-9b level in NSCLC cells by down-regulating the expression of caspase-9b or modulating the alternative splicing of caspase-9 pre-mRNA to favor the formation of caspase-9a instead of caspase-9b. The significance of therapies targeting caspase-9b or caspase-9b-cIAP1

interaction is the specificity for cancer/tumor cells as cascape-9b is unnoticeably expressed in non-transformed cells (21). In other words, utilization of caspase-9b-targeting approach is ideal for cancer-specific treatment. Although NF-κB inhibitors have been shown to be promising for therapeutic treatment against cancer, there is a serious concern about using NF-κB inhibitors in cancer therapy: suppressing the NF-κB signaling may impair immunity since NF-κB pathways play crucial roles in both innate and adaptive immunity. Hence, caspase-9b-targeting approach for restricting canonical NF-κB activation would not only be cancer-specific but also address the main problem associated with using NF-κB inhibitors in cancer treatment: therapies preventing caspase-9b-mediated NF-κB activation would affect the NF-κB signaling only in tumor cells but not in normal cells and thereby, have a limited effect on the immunity.

c-IAP1 was identified as a key factor mediating the mechanistic and biological roles of caspase-9b in the NF-κB pathways. Interesting, depletion of c-IAP2, a closely related IAP to c-IAP1, was not shown to affect the activating/inhibitory roles of caspase-9b on the NF-κB pathways (figure 2.13). Also, c-IAP2 did not compensate for the loss of c-IAP1; specifically, elevated level of c-IAP2 as a consequence of c-IAP1 down-regulation (figure 2.14A) did not 'rescue' the blocking effect of cIAP1 down-regulation on caspase-9b-mediated reduction of IκB-α and NIK level or ubiquitination of RIP1 and NIK (figure 2.7). Many reports have pointed out the critical roles of c-IAPs in the NF-κB signaling; however, it has not been well-documented whether exclusive c-IAP1 or c-IAP2 or both c-IAPs play(s) roles in the NF-κB pathways and in which circumstances and whether redundant compensatory roles exist between c-IAP1 and c-IAP2. With respect to the facilitating functions for caspase-9b in the NF-κB pathways, this study ruled out the redundant roles between two c-IAPs and highlighted the exclusive roles of c-IAP1 but not c-IAP2.

The IBM on caspase-9b and and D320 residue in BIR3 domain of c-IAP1 was identified to be essential for the interaction between caspase-9b and c-IAP1. Interestingly, despite being reported to be important for caspase-9 binding (16), mutation at this residue has not been shown to affect c-IAP1 binding to another IBM-containing protein, Smac/DIABLO (54). Three other mutations in BIR2 or BIR3 of c-IAP1 have also been utilized in this study and all of these mutations have been reported to disrupted c-IAP1 binding to caspase-9 or Smac/DIABLO (16, 54). However, none of these mutations were observed to decrease c-IAP1 binding to caspase-9b (figure 2.10). Another interesting finding regarding c-IAP1/caspase-9b interaction is that caspase-9b does not need to be cleaved to binds to c-IAP1 as caspase-9 (figure 2.9). The differences in binding mode between c-IAP1/caspase-9b and c-IAP1-/caspase-9 can be explained by the possibility that truncated caspase-9b has an altered configuration compared to full-size caspase-9, which still interacts with c-IAP1 at BIR3 domain but at different residues and is no longer required processing to expose its IBM for binding to c-IAP1.

Caspase-9b binds to c-IAP1 and enhances its E3 ligase activity for canonical NF-κB activation or noncanonical NF-κB supression. A remaining question is how this interaction with caspase-9b augments the E3 ligase activity of c-IAP1. Given that the CARD domain on c-IAP1 can autoinhibit its E3 activity by preventing the RING dimerization and blocking the access to E2 activating enzyme (43), association with caspase-9b might change the conformation of c-IAP1 from inactive to active form, which would no longer be affected by CARD-mediated autoinhibition. This hypothesis could be addressed by further determination of c-IAP1 structure in the binding configuration with caspase-9b.

Here we have revealed that caspase-9b exhibits opposing functions in the NF-κB pathways in a NSCLC cell line, A549 (wild-type p53 and mutant Kras genotype). The activating roles of

caspase-9b in the canonical NF-κB pathway also translated to another NSCLC cell line, H838 (wild-type p53 and wild-type K-ras genotype) and nontransformed bronchial epithelial primary cell line, HBEpC (figure 2.15). However, caspase-9b was not shown to affect the non-canonical pathway in either H838 or HBEpC (figure 2.15). This observation could be explained by another observation that non-canonical activation is undetectable or relatively low in HBEpC and H838 compared to A549 cells (figure 2.16). Also, it is likely that the noncanonical pathway might negatively impact the canonical activation. In other words, caspase-9b suppresses the noncanonical pathway to favor the canonical activation and in cases of cells with noncanonical activation at lower level than the basal level for suppressing the canonical pathway, inhibition of the noncanonical pathway might be unnecessary.

Based on this study, down-regulation of c-IAP1 resulted in similar outcomes as down-regulation of caspase-9b, particularly the effects on NF-κB pathways (figure 2.6), which supports the idea regarding cooperation between c-IAP1 and caspase-9b in regulation of NF-κB signaling. Nonetheless, different from caspase-9b, which was demonstrated to promote cell survival, c-IAP1 reduction did not alter the viability of NSCLC cells (figure 2.7). Since c-IAP1 depletion was shown to remarkably increase c-IAP2 level (figure 2.14A), it is likely that c-IAP2 activates other survival pathways or inhibits cell death pathways in a NF-κB-independent manner to compensate for the loss of c-IAP1. However, this possibility was ruled out by the observation that down-regulation of caspase-9b also led to an increase in c-IAP2 level (figure 2.14B). Therefore, another possible and more likely explanation for the difference between c-IAP1 and caspase-9b with respects to the effects on cell survival is based on the anti-apoptotic function of caspase-9b besides its roles in NF-κB signaling. In the absence of c-IAP1 for canonical NF-κB

activation to maintain cell survival, caspase-9b might help protect cells from undergoing apoptosis by preventing the activation of caspase-9 and down-stream caspase cascade.

The canonical NF-kB pathway has been shown to be important for the development of Kras-induced lung tumor (2). It is plausible that by activating the canonical NF-kB, caspase-9b might facilitate Kras-mediated lung tumor formation. Therefore, our future effort will focus on determining if caspase-9b cooperates with KRAS mutation to drive tumorigenesis in mouse model. Specifically, adenovirus expressing caspase-9b will be delivered to the mutant $Kras^{G12V}$ transgenic mice to examine whether expression of caspase-9b augments the enhancing effect of KRAS mutation on tumoregenesis. If we could validate this hypothesis, targeting caspase-9b would be an attractive anti-NSCLC approach for patients carrying KRAS mutation.

This study has pointed to the importance of caspase-9b/cIAP1 interaction for tumorigenicity of NSCLC cells. Hence, identification of compounds that prevent the binding of caspase-9b to cIAP1 would be a potential approach for development of chemotherapeutic drugs to treat NSCLC, which is also our future direction besides validating the proposed hypothesis regarding the cooperation between caspase-9b and *KRAS* mutation on tumorigenesis. Specifically, we will perform high throughput screening (HTS) for drug compounds that interferes with caspase-9b/c-IAP1 binding. The first step in this process will be identification and optimization of a high throughput assay that allows specific measurement of caspase-9b/cIAP1 interaction.

Literature cited

1. Basak, S., Kim, H., Kearns, J. D., Tergaonkar, V., O'Dea, E., Werner, S. L., Benedict, C. A., Ware, C. F., Ghosh, G., Verma, I. M. A fourth IkappaB protein within the NF-kappaB signaling module. *Cell* 128:369-381 (2007).
2. Bassères D. S., Ebbs A., Levantini E., Baldwin A. S. Requirement of the NF-kappaB subunit p65/RelA for K-Ras-induced lung tumorigenesis. *Cancer Res*. 70:3537-3546 (2010).
3. Berglund F. M., Clarke P. R. hnRNP-U is a specific DNA-dependent protein kinase substrate phosphorylated in response to DNA double-strand breaks. *Biochem. Biophys. Res. Commun.* 381:59-64 (2009).
4. Bertrand M. J., Lippens S., Staes A., Gilbert B., Roelandt R., De Medts J., Gevaert K., Declercq W., Vandenabeele P. cIAP1/2 are direct E3 ligases conjugating diverse types of ubiquitin chains to receptor interacting proteins kinases 1 to 4 (RIP1-4). *PLoS One.* 6:e22356 (2011).
5. Bertrand M. J., Milutinovic S., Dickson K. M., Ho W. C., Boudreault A., Durkin J., Gillard J. W., Jaquith J. B., Morris S. J., Barker P. A... cIAP1 and cIAP2 facilitate cancer cell survival by functioning as E3 ligases that promote RIP1 ubiquitination. *Mol Cell*. 30:689–700 (2008).

6. Britton S., Froment C., Frit P., Monsarrat B., Salles B., Calsou P. Cell nonhomologous end joining capacity controls SAF-A phosphorylation by DNA-PK in response to DNA double-strand breaks inducers. *Cell Cycle.* **8**:3717-22 (2009).
7. Burke S. P., Smith L., Smith J. B. cIAP1 cooperatively inhibits procaspase-3 activation by the caspase-9 apoptosome. *J Biol Chem*. 285:30061-30068 (2010).
8. Chalfant C. E., Rathman K., Pinkerman R. L., Wood R. E., Obeid L. M., Ogretmen B., Hannun Y. A. De novo ceramide regulates the alternative splicing of caspase-9 and Bcl-x in A549 lung adenocarcinoma cells. Dependence on protein phosphatase-1. *J. Biol. Chem.* 277:12587-12595 (2002).
9. Chaudhary P. M., Eby M. T., Jasmin A., Kumar A., Liu L., Hood L. Activation of the NF-kappaB pathway by caspase 8 and its homologs. *Oncogene.* 19:4451-4460 (2000).
10. Chen F., Lu Y., Zhang Z., Vallyathan V., Ding M., Castranova V. and Shi X. Opposite effect of NF-kappa B and c-Jun N-terminal kinase on p53-independent GADD45 induction by arsenite. *J Biol Chem*. 276:11414-11419 (2001).
11. Chen L. M., Kuo C. H., Lai T. Y., Lin Y. M., Su C. C., Hsu H. H., Tsai F. J., Tsai C. H., Huang C. Y., Tang C. H. RANKL increases migration of human lung cancer cells through intercellular adhesion molecule-1 up-regulation. *J Cell Biochem*. 112:933-941 (2011).
12. Chen W, Li Z, Bai L, Lin Y. NF-kappaB in lung cancer, carcinogenesis mediator and a prevention and therapy target. *Front Biosci*. 16:1172-1185 (2011).
13. D'Amato T. A., Landreneau R. J., McKenna R.J., Santos R. S., Parker R.J. Prevalence of *in vitro* extreme chemotherapy resistance in resected non-small cell lung cancer. *Ann Thorac Surg*. 81:440–447 (2006).

14. Deng J., Fujimoto J., Ye X. F., Men T. Y., Van Pelt C. S., Chen Y. L., Lin X. F., Kadara H., Tao Q., Lotan D. and Lotan R. Knockout of the tumor suppressor gene Gprc5a in mice leads to NF-kappaB activation in airway epithelium and promotes lung inflammation and tumorigenesis. *Cancer Prev Res*. 3:424-437 (2010).
15. Ea, C. K., Deng, L., Xia, Z. P., Pineda, G. and Chen, Z. J.. Activation of IKK by TNFalpha requires site-specific ubiquitination of RIP1 and polyubiquitin binding by NEMO. *Mol. Cell.* 22:245-257 (2006).
16. Eckelman B. P., Salvesen G. S. The human anti-apoptotic proteins cIAP1 and cIAP2 bind but do not inhibit caspases. *J Biol Chem*. 281:3254-3260 (2006)
17. Eggert M., Michel J., Schneider S., Bornfleth H., Baniahmad A., Fackelmayer F. O., Schmidt S, Renkawitz R. The glucocorticoid receptor is associated with the RNA-binding nuclear matrix protein hnRNP U. *J. Bio. Chem.* 272:28471-28478 (1997).
18. Elmore S. Apoptosis: a review of programmed cell death. *Toxicol Pathol.* 35:495-516 (2007).
19. Fackelmayer F. O., Dahm K., Renz A., Ramsperger U., Richter A. Nucleic-acid-binding properties of hnRNP-U/SAF-A, a nuclear-matrix protein which binds DNA and RNA in vivo and in vitro. *Eur. J. Biochem.* 221:749-757 (1994).
20. Fu D., Collins K. Purification of human telomerase complexes identifies factors involved in telomerase biogenesis and telomere length regulation. *Mol. Cell*. 28:773-785 (2007*).*
21. Goehe R. W., Shultz J. C., Murudkar C., Usanovic S., Lamour N. F., Massey D. H., Zhang L., Camidge D. R., Shay J. W., Minna J. D., Chalfant C. E. hnRNP L regulates the tumorigenic capacity of lung cancer xenografts in mice via caspase-9 pre-mRNA processing. *J Clin Invest*. 120:3923-3939 (2010).

22. Grivennikov S. I., Greten F. R. and Karin M. Immunity, inflammation and cancer. *Cell*. 140:883-899 (2010).

23. Hasegawa Y., Brockdorff N., Kawano S., Tsutui K., Tsutui K., Nakagawa S. The matrix protein hnRNP U is required for chromosomal localization of Xist RNA. *Dev. Cell.* 19:469–476 (2010).

24. Hayden M. S., Ghosh S. Shared principles in NF-kappaB signaling. *Cell*. 132:344-362 (2008).

25. Helbig R., Fackelmayer F. O. Scaffold attachment factor A (SAF-A) is concentrated in inactive X chromosome territories through its RGG domain. *Chromosoma* 112:173–182 (2003).

26. Hinz M., Krappmann D., Eichten A., Heder A., Scheidereit C., Strauss M. NF-kappaB function in growth control: reg.lation of cyclin D1 expression and G0/G1-to-S-phase transition. *Mol Cell Biol*. 19:2690-2698 (1999).

27. Huang C. Y., Fong Y. C., Lee C. Y., Chen M. Y., Tsai H. C., Hsu H. C. and Tang C. H. CCL5 increases lung cancer migration via PI3K, Akt and NF-kappaB pathways. *Biochem Pharmacol*. 77:794-803 (2009).

28. Jin H. S., Lee D. H., Kim D. H., Chung J. H., Lee S. J., Lee T. H. cIAP1, cIAP2, and XIAP act cooperatively via nonredundant pathways to regulate genotoxic stress-induced nuclear factor-kappaB activation. *Cancer Res.* 69:1782-1791 (2009)

29. Jin X., Wang Z., Qiu L., Zhang D., Guo Z., Gao Z., Deng C., Wang F., Wang S. and Guo C. Potential biomarkers involving IKK/RelA signal in early stage non-small cell lung cancer. *Cancer Sci*. 99z;582-589 (2008).

30. Jones D. R., Broad R. M., Madrid L. V., Baldwin A. S., Mayo M.W. Inhibition of NF-κB sensitizes non-small cell lung cancer cells to chemotherapy-induced apoptosis. *Ann Thorac Surg*. 70:930-937 (2000).
31. Karin M. and Greten F. R. NF-kappaB: linking inflammation and immunity to cancer development and progression. *Nat Rev Immunol*. 5:749-759 (2005).
32. Karin M. and Lin A. NF-kappaB at the crossroads of life and death. *Nat Immunol*. 3:221-227 (2002).
33. Kelliher, M. A., Grimm, S., Ishida, Y., Kuo, F., Stanger, B. Z. and Leder, P. The death domain kinase RIP mediates the TNF-induced NF-kappaB signal. *Immunity*. 8:297-303 (1998).
34. Kiledjian M., Dreyfuss G. Primary structure and binding activity of the hnRNP U protein: binding RNA through RGG box. *EMBO J.* 11:2655-2664 (1992).
35. Kim M. K., Nikodem V. M. hnRNP U inhibits carboxy-terminal domain phosphorylation by TFIIH and represses RNA polymerase II elongation. *Mol. Cell Biol.* 19:6833-6844 (1999).
36. Kukalev A., Nord Y., Palmberg C., Bergman T., Percipalle P. Actin and hnRNP U cooperate for productive transcription by RNA polymerase II. *Nat. Struct. Mol. Biol.* 12:238–244 (2005).
37. Lamkanfi M., Kalai M., Saelens X., Declercq W., Vandenabeele P. Caspase-1 activates nuclear factor of the kappa-enhancer in B cells independently of its enzymatic activity. *J Biol Chem*. 279:24785-24793 (2004).
38. Lamkanfi, M., D'Hondt K., Vande Walle L., Van Gurp M., Denecker G., Demeulemeester J., Kalai M., Declercq W., Saelens X. and Vandenabeele P. A novel caspase-2 complex containing TRAF2 and RIP1. *J. Biol. Chem*. 280:6923–6932 (2005).

39. Lawrence, T., Bebien, M., Liu, G. Y., Nizet, V. and Karin, M. IKKalpha limits macrophage NF-kappaB activation and contributes to the resolution of inflammation. *Nature.* 434: 1138-1143 (2005).

40. Li J., Jia H., Xie L., Wang X., He H., Lin Y. and Hu L. Association of constitutive nuclear factor-kappaB activation with aggressive aspects and poor prognosis in cervical cancer. *Int J Gynecol Cancer*. 19:1421-1426 (2009).

41. Liao G., Zhang M., Harhaj E. W., Sun S. C. Regulation of the NFkappaB-inducing kinase by tumor necrosis factor receptorassociated factor 3-induced degradation. *J Biol Chem*. 279:26243-26250 (2004).

42. Lin Y., Bai L., Chen W. and Xu S. The NF-kappaB activation pathways, emerging molecular targets for cancer prevention and therapy. *Expert Opin Ther Targets*, 14:45-55 (2010).

43. Lopez J., John S. W., Tenev T., Rautureau G. J., Hinds M. G., Francalanci F., Wilson R., Broemer M., Santoro M. M., Day C. L., Meier P. CARD-mediated autoinhibition of cIAP1's E3 ligase activity suppresses cell proliferation and migration. *Mol Cell*. 42:569-583 (2011).

44. Mahoney D. J., Cheung H. H., Mrad R. L., Plenchette S., Simard C., Enwere E., Arora V., Mak T. W., Lacasse E. C., Waring J., Korneluk R. G. Both cIAP1 and cIAP2 regulate TNFa-mediated NF-κB activation. *Proc Natl Acad Sci*. 105:11778–11783 (2008).

45. Massiello A., Chalfant C. E. SRp30a (ASF/SF2) regulates the alternative splicing of caspase-9 pre-mRNA and is required for ceramide-responsiveness. *J. Lipid Res.* 47:892–897 (2006).

46. Matunis M. J., Michael W. M., Dreyfuss G. Characterization and primary structure of the poly(C)-binding heterogeneous nuclear ribonucleoprotein complex K protein. *Mol. Cell Biol.* 12:164-171 (1992).

47. Meylan E., Dooley A. L., Feldser D. Shen M., L., Turk E., Ouyang C. and Jacks T. Requirement for NFkappaB signalling in a mouse model of lung adenocarcinoma. *Nature.* 462:104-107 (2009).

48. Mi J., Zhang X., Liu Y., Reddy S. K., Rabbani Z. N., Sullenger B. A. and Clary B. M. NF-kappaB inhibition by an adenovirus expressed aptamer sensitizes TNFalpha-induced apoptosis. *Biochem Biophys Res Commun*. 359:475-480 (2007).

49. Mi J., Zhang X., Rabbani Z. N., Liu Y., Reddy S. K., Su Z., Salahuddin F. K., Viles K., Giangrande P. H., Dewhirst M. W., Sullenger B. A., Kontos C. D., Clary B. M. RNA aptamer-targeted inhibition of NF-kappa B suppersses non-small cell lung cancer resistance to doxorubicin. *Mol Ther*. 16:66-73 (2008).

50. Molina J. R., Yang P., Cassivi S. D., Schild S. E., Adjei A. Non-small cell lung cancer: Epidemiology, risk factors, treatment and survivorship. *Mayo Clin Proc*. 83:584–594 (2008).

51. Motta-Mena L. B., Heyd F., Lynch K. W. Context-dependent regulatory mechanism of the splicing factor hnRNP L. *Mol. Cell.* 37:223-234 (2010).

52. Nakanishi C. and Toi M. Nuclear factor-kappaB inhibitors as sensitizers to anticancer drugs. *Nat Rev Cancer*. 5:297-309 (2005).

53. Obrdlik A., Kukalev A., Louvet E., Farrants A. K., Caputo L., Percipalle P. The histone acetyltransferase PCAF associates with actin and hnRNP U for RNA polymerase II transcription. *Mol. Cell. Biol.* 28:6342–6357 (2008).

54. Samuel T., Welsh K., Lober T., Togo S.H., Zapata J. M., Reed J. C. Distinct BIR domains of cIAP1 mediate binding to and ubiquitination of tumor necrosis factor receptor-associated factor 2 and second mitochondrial activator of caspases. *J Biol Chem.* 281:1080-1090 (2006).

55. Seol D-W. & Billiar T. A caspase-9 variant missing the catalytic site Is an endogenous inhibitor of apoptosis. *J. Biol. Chem*. 274:2072-2076 (1999).

56. Shikama, Y., M. Yamada and T. Miyashita. Caspase-8 and caspase-10 activate NF-kappaB through RIP, NIK and IKKalpha kinases. *Eur. J. Immunol*. 33:1998–2006 (2003).

57. Shultz J. C., Goehe R. W., Wijesinghe D. S., Murudkar C., Hawkins A. J., Shay J. W., Minna J. D., Chalfant C. E. Alternative splicing of caspase-9 is modulated by the phosphoinositide 3-kinase/Akt pathway via phosphorylation of SRp30a. *Cancer Res.* **70**:9185-9196 (2010).

58. Shultz J. C., Goehe R. W., Murudkar C. S., Wijesinghe D. S., Mayton E. K., Massiello A., Hawkins A. J., Mukerjee P., Pinkerman R. L., Park M. A., Chalfant C. E. SRSF1 regulates the alternative splicing of caspase-9 via a novel intronic splicing enhancer affecting the chemotherapeutic sensitivity of non-small cell lung cancer cells. *Mol. Cancer Res.* 9:889-900 (2011).

59. Srinivasula S.M., Ahmad M., Guo Y., Zhan Y., Lazebnik Y., Fernandes-Alnemri T. & Alnemri E. S. Identification of an endogenous dominant-negative short isoform of caspase-9 that can regulate apoptosis. *Cancer Res*. 59:999-1002(1999).

60. Srinivasula S. M., Hegde R., Saleh A., Datta P., Shiozaki E., Chai J., Lee R. A., Robbins P. D., Fernandes-Alnemri T., Shi Y., Alnemri E. S. A conserved XIAP-interaction motif in caspase-9 and Smac/DIABLO regulates caspase activity and apoptosis. *Nature*. 410:112-116 (2001).

61. Stephanou A., Scarabelli T. M., Knight R. A., Latchman D. S. Antiapoptotic activity of the free caspase recruitment domain of procaspase-9: a novel endogenous rescue pathway in cell death. *J Biol Chem*. 277:13693-13699 (2002).

62. Trapnell C., Williams B. A., Pertea G., Mortazavi A. M., Kwan G., van Baren M. J., Salzberg S. L., Wold B., Pachter L. Transcript assembly and abundance estimation from RNA-Seq reveals thousands of new transcripts and switching among isoforms. *Nat Biotechnol*. 28:511–515 (2010).
63. Vallabhapurapu S., Matsuzawa A., Zhang W., Tseng P. H., Keats J. J., Wang H., Vignali D. A., Bergsagel P. L., Karin M. Nonredundant and complementary functions of TRAF2 and TRAF3 in a ubiquitination cascade that activates NIK-dependent alternative NF-kappaB signaling. *Nat Immunol.* 9:1364-1370 (2008).
64. Vallabhapurapu S., Karin M. Regulation and function of NFkappaB transcription factors in the immune system. *Annu Rev Immunol*. 27:693-733 (2009).
65. Varfolomeev E., Blankenship J. W., Wayson S. M., et al. IAP antagonists induce autoubiquitination of c-IAPs, NF-kappaB activation and TNFalpha-dependent apoptosis. *Cell*. 131:669–681 (2007).
66. Wang C. Y., Cusack J. C. Jr, Liu R., Baldwin A. S. Jr. Control of inducible chemoresistance: enhanced anti-tumor therapy through increased apoptosis by inhibition of NF-κB. *Nat Med*. 5:412-417 (1999).
67. Wu, C. J., Conze, D. B., Li, T., Srinivasula, S. M. and Ashwell, J. D. Sensing of Lys 63-linked polyubiquitination by NEMO is a key event in NF-kappaB activation [corrected]. *Nat. Cell Biol.* 8:398-406 (2006).
68. Yugami M., Kabe Y., Yamaguchi Y., Wada T., Handa H. hnRNP-U enhances the expression of specific genes by stabilizing mRNA. *FEBS Lett.* 581:1-7 (2007).

69. Xiao R., Tang P., Yang B., Huang J., Zhou Y., Shao C., Li H., Sun H., Zhang Y., Fu X. D. Nuclear matrix factor hnRNP U/SAF-A exerts a global control of alternative splicing by regulating U2 snRNP maturation. *Mol. Cell.* 45:656-668 (2012).

70. Youlden D. R., Cramb S. M., Baade P. D. The international epidemiology of lung cancer: Geographical distribution and secular trends. *J Thorac Oncol*. 3:819–831 (2008).

71. Zarnegar B. J., Wang Y., Mahoney D. J., Dempsey P. W., Cheung H. H., Shiba He J., T., Yang X., Yeh W. Mak C., T. W., Korneluk R. G. and Cheng G. Non-canonical NF-kappaB activation requires coordinatedassembly of a regulatory complex of the adaptors cIAP1, cIAP2, TRAF2 and TRAF3 and the kinase NIK. *Nat Immunol*. 9:1371-1378 (2008).